

Title	Bioinspired aryldiazonium carbohydrate coatings: reduced adhesion of foulants at polymer and stainless steel surfaces in a marine environment
Authors	Myles, Adam;Haberlin, Damien;Esteban-Tejeda, Leticia;Angione, M. Daniela;Browne, Michelle P.;Hoque, Md Khairul;Doyle, Thomas K.;Scanlan, Eoin M.;Colavita, Paula E.
Publication date	2017-12-04
Original Citation	Myles, A., Haberlin, D., Esteban-Tejeda, L., Angione, M. D., Browne, M. P., Hoque, M. K., Doyle, T. K., Scanlan, E. M. and Colavita, P. E. (2017) 'Bioinspired aryldiazonium carbohydrate coatings: reduced adhesion of foulants at polymer and stainless steel surfaces in a marine environment', ACS Sustainable Chemistry and Engineering, 6(1), pp. 1141-1151. doi:10.1021/acssuschemeng.7b03443
Type of publication	Article (peer-reviewed)
Link to publisher's version	10.1021/acssuschemeng.7b03443
Rights	© 2017, American Chemical Society. This document is the Accepted Manuscript version of a Published Work that appeared in final form in ACS Sustainable Chemistry and Engineering, © American Chemical Society, after peer review and technical editing by the publisher. To access the final edited and published work see https://pubs.acs.org/doi/abs/10.1021/acssuschemeng.7b03443
Download date	2024-09-10 09:21:34
Item downloaded from	https://hdl.handle.net/10468/7132



UCC

University College Cork, Ireland
Coláiste na hOllscoile Corcaigh

Article

Bioinspired Aryldiazonium Carbohydrate Coatings: Reduced Adhesion of Foulants at Polymer and Stainless Steel Surfaces in a Marine Environment

Adam Thomas Myles, Damien Haberlin, Leticia Esteban-Tejeda, M. Daniela Angione, Michelle P. Browne, Md. Khairul Hoque, Thomas K Doyle, Eoin M. Scanlan, and Paula E. Colavita

ACS Sustainable Chem. Eng., **Just Accepted Manuscript** • DOI: 10.1021/acssuschemeng.7b03443 • Publication Date (Web): 04 Dec 2017

Downloaded from <http://pubs.acs.org> on December 13, 2017

Just Accepted

“Just Accepted” manuscripts have been peer-reviewed and accepted for publication. They are posted online prior to technical editing, formatting for publication and author proofing. The American Chemical Society provides “Just Accepted” as a free service to the research community to expedite the dissemination of scientific material as soon as possible after acceptance. “Just Accepted” manuscripts appear in full in PDF format accompanied by an HTML abstract. “Just Accepted” manuscripts have been fully peer reviewed, but should not be considered the official version of record. They are accessible to all readers and citable by the Digital Object Identifier (DOI®). “Just Accepted” is an optional service offered to authors. Therefore, the “Just Accepted” Web site may not include all articles that will be published in the journal. After a manuscript is technically edited and formatted, it will be removed from the “Just Accepted” Web site and published as an ASAP article. Note that technical editing may introduce minor changes to the manuscript text and/or graphics which could affect content, and all legal disclaimers and ethical guidelines that apply to the journal pertain. ACS cannot be held responsible for errors or consequences arising from the use of information contained in these “Just Accepted” manuscripts.

1
2
3 **Bioinspired Aryldiazonium Carbohydrate Coatings: Reduced Adhesion of**
4
5 **Foulants at Polymer and Stainless Steel Surfaces in a Marine Environment**
6
7

8 Adam Myles,^a Damien Haberlin,^b Leticia Esteban-Tejeda,^a M. Daniela Angione,^a Michelle P.
9 Browne,^a Md. Khairul Hoque,^a Thomas K. Doyle,^c Eoin M. Scanlan^{a*} and Paula E. Colavita^{a*}
10
11
12

13
14 ^a School of Chemistry, CRANN and AMBER Research Centres, Trinity College Dublin, College
15 Green, Dublin 2, Ireland
16
17

18
19 ^b Marine and Renewable Energy Centre, Environmental Research Centre, University College
20 Cork, Beaufort Building, Haulbowline Road, Ringaskiddy, Cork, Ireland
21
22

23
24 ^c School of Natural Sciences (Zoology), Ryan Institute and Marine and Renewable Energy
25 Centre, National University of Ireland Galway, Galway, Ireland
26
27
28

29
30 * Corresponding: colavitp@tcd.ie and eoin.scanlan@tcd.ie
31
32
33
34
35
36
37
38
39
40
41
42
43
44
45
46
47
48
49
50
51
52
53
54
55
56
57
58
59
60

Abstract

Surface treatments that minimise biofouling in marine environments are of interest for a variety of applications, such as environmental monitoring and aquaculture. We report on the effect of saccharide coatings on biomass accumulation at the surface of three materials that find applications in marine settings: stainless steel 316 (SS316), nylon-6 (N-6), and poly(ether sulfone) (PES). Saccharides were immobilized *via* aryldiazonium chemistry; SS316 and N-6 samples were subjected to oxidative surface pre-treatments prior to saccharide immobilization, whereas PES was modified *via* direct reaction of pristine surfaces with the aryldiazonium cations. Functionalization was confirmed by a combination of X-ray photoelectron spectroscopy, contact angle experiments and fluorescence imaging of lectin-saccharide binding. Saccharide immobilization was found to increase surface hydrophilicity of all materials tested, while laboratory tests demonstrate that the saccharide coating results in reduced protein adsorption in the absence of specific protein-saccharide interactions. The performance of all three materials after modification with aryldiazonium saccharide films was tested in the field *via* immersion of modified coupons in coastal waters over a 20 day time period. Results from combined infrared spectroscopy, light microscopy, scanning electron and He-ion microscopy and adenosine-triphosphate content assays show that the density of retained biomass at surfaces is significantly lower on carbohydrate modified samples with respect to unmodified controls. Therefore, functionalization and field test results suggest that carbohydrate aryldiazonium layers could find applications as fouling resistant coatings in marine environments.

Keywords: aryldiazonium, coatings, marine, fouling, functionalization, carbohydrates.

Introduction

Materials immersed in natural waters are typically subject to biofouling, a process that can compromise the integrity of the material or device of interest and result in performance degradation. Structures which are submerged in a marine environment are particularly susceptible to a wide range of opportunistic fouling organisms,¹⁻² and material biofouling and colonization can have a negative impact in a wide range of fields, from marine transport to environmental monitoring and aquaculture.³⁻⁶ Marine biofilms result in major economic and environmental problems, from corrosion and loss of functionality of marine structures and vessels,⁷⁻⁸ to the spread of invasive species⁹ and increased farmed fish mortality.¹⁰⁻¹² Therefore, there is great interest in developing new strategies for preventing and mitigating biofouling in the marine environment, particularly non-toxic or non-biocidal strategies that are environmentally sustainable, commercially scalable and compatible with the modern regulatory landscape.^{1, 3-4, 13}

Biofouling occurs through a complex mechanism that involves multiple processes over a range of time and length scales.¹³ It is proposed that, in the initial stages, the surface rapidly becomes conditioned by the adsorption of small molecules and organic matter, such as small organics, biopolymers and proteinaceous material. Microorganisms then adhere onto this primed surface eventually forming a biofilm onto which larger organisms can attach and subsequently proliferate.⁵ Accumulation of undesired biomass can be minimized by interfering at one or more of these stages of the biofouling cascade. Historic methods of biofilm mitigation involve the use of toxic coatings such as lead-based and organotin paints,¹⁴ which interfere at the micro- and macro-fouling stages. However, due to adverse effects on marine ecosystems, these methods have been phased-out and even use of

1
2
3 alternative paints and coatings based on copper release is under regulatory scrutiny. The
4
5 disruption of quorum sensing signals to inhibit/regulate biofilm formation potentially offers
6
7 a more targeted approach than metal-based biocides; however, this technology is in its
8
9 infancy and its environmental impact on ecosystems remains to be assessed.¹⁵
10

11
12 The most promising non-biocidal strategies, on the contrary, rely on modifying the physico-
13
14 chemical properties of submerged materials to minimise adsorption and adhesion mainly at
15
16 early fouling stages. Regulation of surface roughness, electrostatic charge distribution and
17
18 wetting behaviour have all been investigated as non-biocidal methods.^{13, 16} Bioinspired
19
20 engineered nanotopographies are effective for regulating cell/spore settling; however,
21
22 complex hierarchical patterns are required to repel settling from heterogeneous
23
24 populations,¹⁷ thus posing significant problems for cost-effective scalability. Regulation of
25
26 wetting and spatial control of hydrophobicity at the nanoscale level have also been explored
27
28 as antifouling mechanisms. Low surface free energy and hydrophobic materials and coatings
29
30 have a long history in antifouling technologies and some well-known examples are
31
32 polysiloxanes, fluoropolymers and superhydrophobic coatings.^{1, 6, 13, 18-19} At the other end of
33
34 the spectrum, hydrophilic coatings, such as those based on polyethylene glycols (PEGs)²⁰
35
36 and bioinspired superhydrophilic zwitterionic polymers,²¹⁻²² have similarly demonstrated
37
38 good performance in laboratory tests.
39
40
41
42
43
44

45
46 Surface-immobilized carbohydrates have previously been investigated for the fabrication of
47
48 hydrophilic coatings for biofouling prevention. Carbohydrates represent an interesting
49
50 family of biomolecules because they are environmentally benign and because they are
51
52 highly stable towards oxidation compared to other chemical species such as
53
54 ethyleneglycols.^{18, 20, 23} Previous work has shown that self-assembled monolayers (SAMs) of
55
56
57
58
59
60

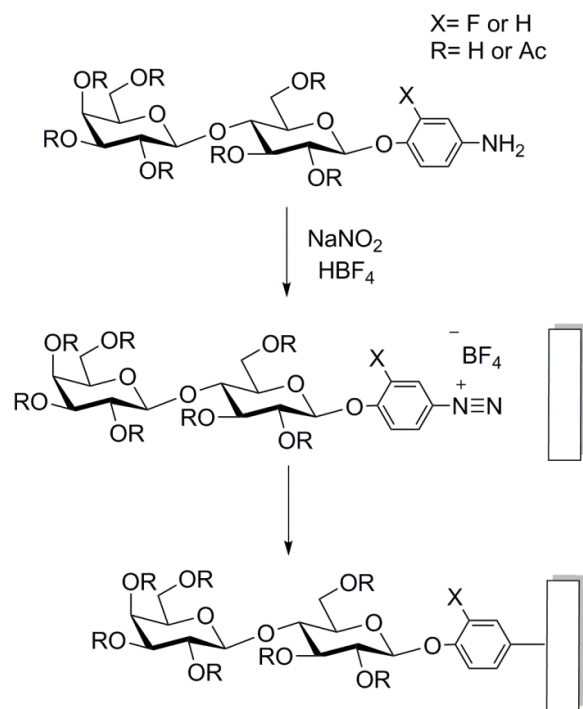
1
2
3 monosaccharides and di-saccharides on gold surfaces can greatly reduce fouling from
4
5 protein solutions.²⁴⁻²⁷ More recently, Ederth et al.²⁵ demonstrated that galactose-bearing
6
7 SAMs were successful at reducing *Ulva linza* spore settling, thus showing promise for marine
8
9 fouling control. Polysaccharides have also been investigated, however the efficient calcium
10
11 binding affinity displayed by many of these, e.g. hyaluronic and pectinic acids, has been
12
13 identified as detrimental for fouling control in the marine environment.²⁸⁻²⁹ Nonetheless,
14
15 relative to other functional coatings, carbohydrates are underexplored in marine
16
17 applications and results from field tests are rare in the literature.
18
19

20
21
22 We have recently shown that aryldiazonium chemistry offers a viable route for the
23
24 immobilization of saccharides at carbon, metal and selected polymer surfaces.³⁰ This
25
26 immobilization strategy can be carried out from solution *via* spontaneous reaction, resulting
27
28 in thin conformal functional films that can be applied *via* flow, spray or dip coating methods
29
30 using aqueous solutions, thus making it attractive and feasible for large scale applications.
31
32 Covalent grafting of mono- and disaccharide-bearing aryldiazonium cations to carbon,
33
34 polydimethylsiloxane (PDMS) and polyethersulfone (PES) was found to significantly reduce
35
36 protein adsorption in laboratory tests.³¹⁻³³ Interestingly, in the case of PES surfaces the
37
38 ability to prevent protein adsorption translated well to field tests, whereby aryldiazonium
39
40 glycoside coatings were found to reduce biomass accumulation after prolonged exposure to
41
42 wastewater effluents.³³ These prior results strongly suggest that aryldiazonium
43
44 carbohydrate coatings could be effective at minimising biofouling in the complex
45
46 environment of natural waters; however, to the best of our knowledge these coatings have
47
48 not been tested in marine settings.
49
50
51
52
53
54
55
56
57
58
59
60

1
2
3 In this work we report a study of the performance of carbohydrates immobilized *via*
4
5 aryldiazonium grafting as fouling resistant coatings on coupons of three different materials
6
7 of technological importance: stainless steel, nylon and PES. Polyamide materials and metal
8
9 alloys are used regularly in the marine environment and are particularly susceptible to
10
11 marine fouling, while PES is a common membrane material used in aquatic sensors.
12
13 Lactosides were chosen for immobilization *via* spontaneous aryldiazonium grafting, because
14
15 of their lack of calcium-binding carboxylic acid residues,²⁸ and on the basis of previously
16
17 published comparative tests on the performance of simple glycosides.^{24, 32-33} First, we report
18
19 on the effectiveness of spontaneous functionalization reactions on the above substrates;
20
21 second, we report the results of immersion tests in a coastal environment for 20 days over
22
23 the summer period. Results from field tests indicate that carbohydrate coatings show
24
25 promise as a sustainable and environmentally benign approach for reducing adhesion and
26
27 retention of marine foulants.
28
29
30
31

32 33 **Experimental Methods**

34
35 **Chemicals and Materials:** Polyamide- Nylon 6 (N6) sheets, marine grade stainless steel 316
36
37 foil (SS316), and Polyethersulfone sheets (PES) were purchased from Goodfellow;
38
39 formaldehyde solution for molecular biology $\geq 36.0\%$ in H₂O, hypophosphorous acid solution
40
41 50%wt. in H₂O, sodium hypochlorite (bleach), sodium hydroxide, potassium hydroxide,
42
43 phosphate buffered saline buffer (0.010 M PBS, pH 7.4), sodium nitrite, hydrochloric acid
44
45 and fluoroboric acid were purchased from Sigma Aldrich. Aquasnap ATP Total Water testing
46
47 strips were purchased from Water Technology Ltd. Bovine Serum Albumin (BSA) conjugates
48
49 with Alexa Fluor 647 were purchased from Biosciences. Bovine Serum Albumin (BSA) and
50
51 peanut agglutinin from *Arachis Hypogaea* (PNA) conjugates with fluorescein isothiocyanate
52
53 (FITC)
54
55
56
57
58
59
60



Scheme 1. 4-aminophenol- β -D-lactopyranose compounds used for all functionalized samples and reaction protocol used for diazotization and functionalization with aryldiazonium cations in situ.

were purchased from Sigma Aldrich. 4-aminophenol- β -D-lactopyranose and its fluorinated analogue 2-fluoro-4-aminophenol- β -D-lactopyranose (Scheme 1) were synthesized as previously described.^{30,33} The peracetylated lactoside 2-fluoro-4-aminophenyl-2,3,4,6-tetra-O-acetyl- β -D-galactopyranosyl-(1 \rightarrow 4)-2,3,6-tri-O-acetyl- β -D-glucopyranoside (Scheme 1) was used for infrared experiments; synthesis and characterisation of this compound are reported in the Supplementary Information.

Surface modification: Prior to modification with aryldiazonium cations, both polyamide and stainless steel surfaces were pre-activated, while PES surfaces did not require pre-activation³³ and were used after light cleaning in methanol only. Nylon-6 (N6) samples were pre-activated by overnight immersion at 30 °C in a 36% aqueous formaldehyde solution with a catalytic amount of hypophosphorous acid. Stainless Steel samples (SS316) were pre-

1
2
3 treated with 0.5% NaClO in basic aqueous solution (KOH 1% and NaOH 1%);³² surfaces were
4
5 immersed three times in fresh solution for 10 min at room temperature. Samples were
6
7 rinsed thoroughly with deionized water and functionalized *via* immersion in freshly
8
9 prepared 1.0 mM solutions of aryldiazonium cations generated *in situ* from the
10
11 corresponding amine, 4-aminophenol- β -D-lactopyranose (Scheme 1), following previously
12
13 published protocols.³⁰ Briefly, a 1.25 mM solution of the 4-aminophenol in 0.00150 M HBF₄
14
15 was prepared and cooled to 4 °C or less in an ice bath for 1 h. The cold precursor solution
16
17 was prepared and cooled to 4 °C or less in an ice bath for 1 h. The cold precursor solution
18
19 was diluted via addition of a 0.010 M NaNO₂ to a final concentration of 0.0010 M in 4-
20
21 aminophenol precursor, acid and nitrite. Samples were immersed immediately into the
22
23 precursor solution and kept in the dark for 1 h, then rinsed with deionized water and kept
24
25 under wet storage in deionized water prior to further testing. For field studies a typical
26
27 batch size for material modification was 3 L, while laboratory experiments involved the
28
29 preparation of 25 mL solutions. Functionalization using peracetylated precursors followed
30
31 the same protocol except for the use of acetonitrile as a solvent; samples were rinsed using
32
33 sonication in acetonitrile/methanol, a protocol that had been shown to be effective at
34
35 removing physisorbed acetylated aryldiazonium glycosides.³⁰
36
37
38
39

40 **Surface Characterization:** Water contact angles (WCA) were determined for all samples
41
42 using the sessile drop method (FTA1000), using 20 μ L droplets. Infrared reflectance
43
44 absorption spectroscopy (IRRAS) characterization was carried out on a Bruker Tensor 27
45
46 infrared spectrometer equipped with a mercury cadmium telluride detector and a VeeMax II
47
48 specular reflectance accessory with a wire grid polariser. All spectra were collected using p-
49
50 polarized light; 100 scans at 4 cm⁻¹ were collected for all samples and an unmodified sample
51
52 was used as substrate. X-ray photoelectron spectroscopy (XPS) was carried out on a VG
53
54
55
56
57
58
59
60

1
2
3 Scientific ESCALab MK II system with an Al K α source at 90° takeoff angle. Wide surveys and
4
5 core level spectra were collected at 50 and 20 eV pass energy, respectively. All spectra were
6
7 calibrated to the Cr 2p_{3/2} peak of Cr₂O₃ present in the stainless steel substrate at 576.7 eV
8
9 (Figure S1).³⁴⁻³⁵ Fits were carried out using commercial software (CasaXPS) using Voigt line
10
11 shapes and background correction; atomic ratios were calculated from peak areas after
12
13 correction for relative sensitivity factors (RSF_{C1s} = 1; RSF_{F1s} = 4.43; RSF_{Cr2p} = 11.7; RSF_{Fe2p} =
14
15 16.4). Optical depths were calculated from UV-Vis transmittance measurements (Lambda 35
16
17 Perkin Elmer). Scanning electron microscopy (SEM) images were obtained on a Karl Zeiss
18
19 Ultra Field Emission SEM at accelerating voltages between 2-3 kV in secondary electron
20
21 mode. Helium ion microscopy (HIM) was obtained on a Karl Zeiss NanoFab HIM at 0.2-0.6 pA
22
23 beam currents and 30 kV accelerating voltage, while sample charging was minimized using a
24
25 flood gun.
26
27
28
29
30

31 **Affinity binding and protein adsorption studies *via* fluorescence imaging.** To determine
32
33 protein rejection ability, samples of N6 and SS316 were incubated in 0.2 mg mL⁻¹ solutions
34
35 of BSA fluorescent conjugates in PBS at pH 7.4 for 1 h; Alexa-647 and FITC were the dyes
36
37 used for N6 and SS316, respectively. To determine lectin binding affinity, samples of SS316
38
39 were incubated for 1 h in a 0.2 mg mL⁻¹ solution of PNA-FITC conjugate in pH 7.4 PBS buffer
40
41 with 0.1 mM CaCl₂ and MgCl₂. All samples were washed with PBS solution prior to imaging
42
43 to remove excess unbound protein. Fluorescence images were acquired using an Olympus
44
45 BX51 inverted microscope with cellSense digital image processing software. Emission
46
47 intensities were analysed in triplicate using Image J software.³²
48
49
50
51

52 **ATP determinations:** Adenosine triphosphate (ATP) concentrations per square cm of
53
54 substrate material were determined using the luciferase assay as implemented in a
55
56
57
58
59
60

1
2
3 commercial kit (Aquasnap Total Water).³⁶ The assay was first calibrated using standard
4
5 solutions and the luminometer (Hygiena) to obtain a conversion from relative luminescence
6
7 units (RLU) to ATP concentration (in nM range). Samples of approximately 1 cm² were cut
8
9 from each coupon in triplicate; the cutting was suspended in a known volume of deionized
10
11 water (10 mL or 5 mL, depending on level of fouling) in sterile centrifuge tubes and then
12
13 sonicated for 10 min. The value of RLU was determined for each water sample and
14
15 converted to ATP concentrations; water samples were diluted if needed to bring the ATP
16
17 concentration within the linear range of the assay. Post sonication, the cuttings were dried
18
19 under argon and their mass determined; the relative exposed area was estimated from the
20
21 mass of the cleaned sample cutting and this value was used to surface-normalise ATP
22
23 determinations on individual cutting. Values were compared using ANOVA at 5%
24
25 significance level ($\alpha = 0.05$).
26
27
28
29
30

31 **Coastal Immersion Study:** Immersion studies were carried out on 24th August 2016 in
32
33 Bertraghboy Bay, County Galway, at the site of an unused salmon farming platform
34
35 (Lehanagh pool). Following functionalization, 6 control and 6 functionalized coupons, 100 x
36
37 100 mm² in size, were transported within 24 h under wet storage to the testing site located
38
39 at 150 m from the shore (53.402267°N, 9.820329°W). Polyethylene frames on which N6,
40
41 SS316 and PES coupons had been mounted were set up as shown in Figure 1a. Frames were
42
43 transported by power boat to the testing site and suspended from the edge of the test site
44
45 (Figure 1b) at a depth of approximately 1 m, considered to be optimal for rapid biofouling.³⁷
46
47 The frames were weighted to ensure that all samples would remain in a vertical position
48
49 throughout the duration of the trial which lasted 20 days over the summer months (Aug 24
50
51 – Sept 13). The mean water temperature during the 20 day trial was 16.84 ± 0.31 °C
52
53
54
55
56
57
58
59
60

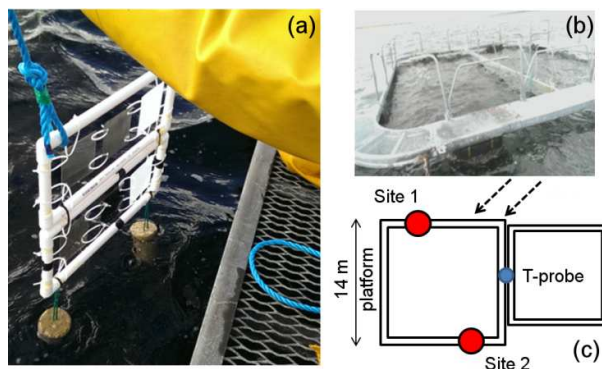


Figure 1. (a) Assembled frame with coupons, arranged from left to right, PES, SS316 and N6, immediately prior to immersion in sea water. (b) Salmon farm platform from which frames with coupons were suspended. (c) Scheme showing the two adjacent platforms and the location of frames at Site 1 and Site 2 relative to the tide (dashed arrows); a temperature probe measured surface water temperature at the position indicated in blue.

(maximum 18.20 °C, minimum 16.23 °C), measured from readings at 1 m depth (StowAway TidbiT). Two positions were chosen for suspending the frames: these are denoted as site 1 and site 2 and are mapped to the platform configuration in Figure 1c. Three samples of each control and functionalized coupon were mounted at each site, i.e. a total of 12 coupons, 4 of each material distributed over the two sites. After the 20 day test, all samples were transported to the laboratory immersed in seawater prior to testing. Samples were rinsed under a stream of deionized water delivered 10 cm above the sample by gravity for 30 s on each side. This procedure was used across all samples to remove loosely attached biomass. Samples were analysed immediately or stored frozen for further characterization.

Results

Aryldiazonium modification of Stainless Steel and Nylon coupons

Coupons of polyethersulfone (PES), stainless steel (SS316) and Nylon-6 (N6) were first modified using lactoside groups *via* spontaneous reaction of aryldiazonium cations to yield

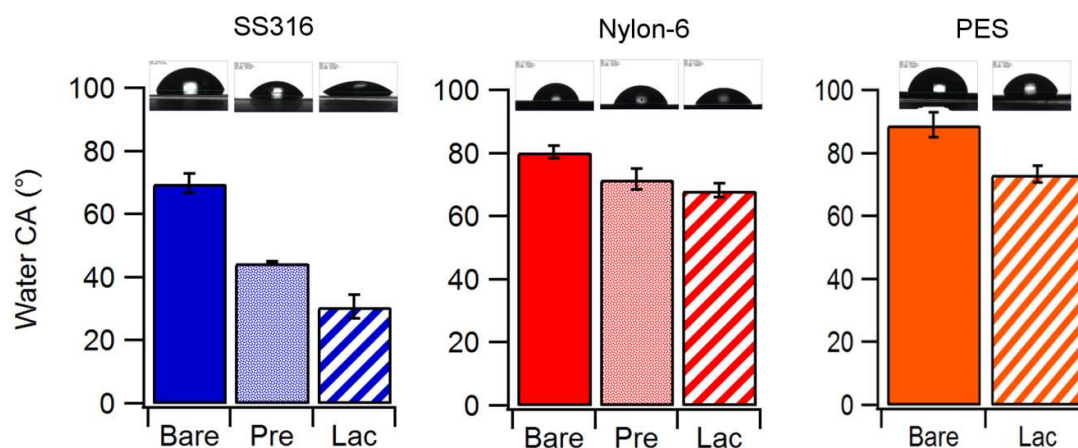


Figure 2. Water contact angle values obtained on bare, pre-treated (except for PES) and Lactose-modified (Lac) surfaces of SS316, Nylon-6 and PES. Samples were pre-activated in caustic bleach and formaldehyde solutions in the case of SS316 and nylon-6, respectively.

surfaces denoted as Lac-PES, Lac-SS and Lac-N6. Aryldiazonium cation solutions were freshly prepared immediately prior to functionalization following standard diazotization protocols; briefly, the arylamine compound was reacted with sodium nitrite in acid aqueous solution at 4 °C (Scheme 1) yielding the corresponding aryldiazonium cation, a highly reactive species.

Work from our group demonstrated that PES undergoes functionalization by spontaneous reaction after immersion of pristine substrates in these solutions and we refer to our previous publication for a full characterization of Lac-PES surfaces thus obtained.³³ In the case of SS316 and N6, surfaces were pre-activated prior to functionalization. SS316 surfaces were pre-activated in caustic hypochlorite (bleach) solutions; this treatment is known to have cleaning and oxidising effects on SS316 surfaces.³⁸⁻⁴⁰ N6 surfaces were pre-treated by immersion in formaldehyde solutions, which are known to activate amide groups in polyamides *via* formation of N-methylol groups.^{36, 41-42} Pre-activation treatments were found to increase surface hydrophilicity as evident from a marked change in water contact angle (Figure 2). The WCA of SS316 decreases from 69.8° to 44.5°, as expected from

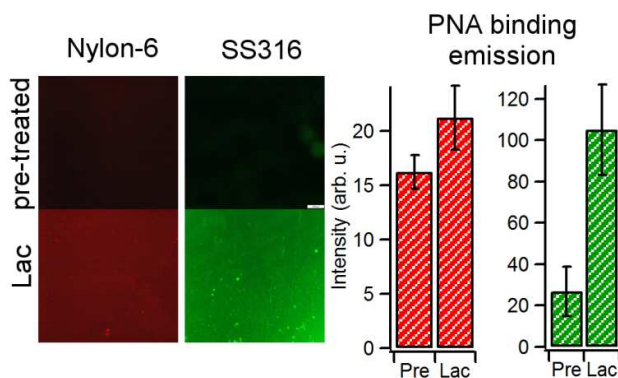


Figure 3. Fluorescence images obtained after lectin binding experiments using dye-conjugated PNA on Nylon-6 and SS316 after pre-treatment and after aryldiazonium modification with lactosides (Lac). The images show that the emission intensity is higher on lactose-modified surfaces. Bar plots represent average emission intensities of Alexa-PNA on Nylon-6 (red bars) and of FITC-PNA on SS316 (green bars) obtained at pre-treated (Pre) and at lactose-modified coupons (Lac).

oxidative cleaning of adventitious organics and exposure of a hydrophilic oxide film.⁴³ The WCA of nylon also decreases from a value of 80.4°, in agreement with literature values for pristine N6, to 71.7°; this is consistent with an increase in the surface density of hydroxyl groups resulting from formaldehyde treatment. Coupons of all three materials tested displayed a significant change in WCA after immersion in the aryldiazonium cation solution. Figure 2 shows that all surfaces decreased their WCA, as expected from the immobilization of hydrophilic saccharide groups and in agreement with previous reports on the effect of lactoside immobilization.³¹

Lactoside immobilization was further confirmed using binding studies using PNA lectin. PNA is known to display binding affinity towards galactose⁴⁴ and can be used to confirm the presence of surface-bound lactosides as these display an available galactose unit at the solid-liquid interface. Lac-SS and Lac-N6 coupons were incubated for 1 h in a solution of fluorescently labeled PNA and rinsed with PBS prior to imaging; Figure 3 shows fluorescence microscopy images of pre-treated and Lac-modified surfaces after PNA incubation and a

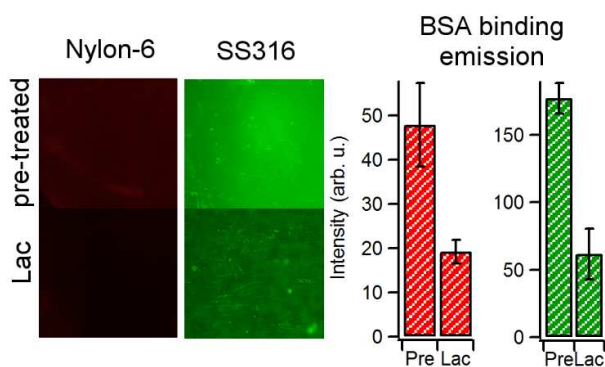


Figure 4. Fluorescence images obtained after protein adsorption experiments using dye-conjugated BSA on Nylon-6 and SS316 after pre-treatment and after aryldiazonium modification with lactosides (Lac). The images show that the emission intensity is lower on lactose-modified surfaces. Bar plots represent average emission intensities of Alexa-BSA on Nylon-6 (red bars) and of FITC-BSA on SS316 (green bars) obtained at pre-treated (Pre) and at lactose-modified coupons (Lac).

comparison of average emission intensities. The stronger emission observed for surfaces after reaction with aryldiazonium cations indicates preferential specific binding with respect to the corresponding bare pre-treated surface and is therefore supporting of functionalization. No evidence of modification was found in the absence of pre-treatment for either SS316 or N6 surfaces.

Protein adsorption experiments were also carried out using fluorescently labeled BSA, a protein that does not display specific binding with glycosides. Figure 4 shows images of pre-treated and Lac-modified SS316 and N6, together with a summary of average emission intensity values obtained using BSA on pre-treated and modified coupons. After functionalization with lactosides a decrease in emission is observed compared to the pre-treated surface, thus indicating that less BSA adsorbs at Lac-SS and Lac-N6 surfaces. This indicates, first, that the increase in fluorescence observed for Lac-SS and Lac-N6 after incubation in PNA solutions is the result of specific Gal-PNA interactions. Second, that immobilization of small saccharides leads to a decrease in unspecific protein binding, in

1
2
3 agreement with observations on the effect of glycoside coatings on carbon and other
4
5 polymer surfaces.^{31,33}
6
7

8 In the case of SS316, functionalization was also confirmed using the fluoro-substituted
9
10 derivative of the lactoside precursor shown in Scheme 1, as the presence of fluorine
11
12 substituents provides good elemental contrast between the functional layer and the bare
13
14 substrate. Survey spectra of pre-treated and modified SS316 in Figure 5a show the
15
16 characteristic peaks of stainless steel associated with Fe 2p, Cr 2p, Ni LMM, O 1s, and C 1s
17
18 lines.⁴⁵⁻⁴⁶ Figures 5b and 5c show the spectra of SS316, in the F 1s and C 1s regions,
19
20 respectively, after pre-treatment and after surface modification in solutions of the
21
22 fluorinated aryldiazonium lactoside.
23
24
25

26
27 Analysis of peak area ratios and fitting of the C 1s line yielded results summarised in Table 1.
28
29 The pre-treated SS316 surface shows C/Cr and Cr/Fe atomic ratios that are consistent with
30
31 those observed for plasma cleaned SS316 by Williams et al.;⁴⁶ the surface was found to be C-
32
33 and Cr-rich with respect to the bulk composition, in agreement with previous compositional
34
35 studies.³⁴ Deconvolution of the C 1s line shows the presence of four main peaks at 285.3 eV
36
37 (C—C and C—H), at 286.8 and 288.7 eV (C—O), and at 289.9 eV (C=O), in agreement with
38
39 previous reports for stainless steel surfaces.⁴⁷ After functionalization, a clear peak is evident
40
41 at 687.0 eV consistent with the F 1s binding energy of fluorinated organics, where F atoms
42
43 are in a low F/C content environment.⁴⁸⁻⁴⁹ Identical changes were obtained in the F 1s
44
45 region after functionalization using chloride as a counterion (Figure S2), thus confirming that
46
47 the F 1s peak does not arise from tetrafluoroborate contamination. Therefore, this result
48
49 suggests that after functionalization the aryl group is bound to the SS316 surface. The
50
51 conclusion is further supported by an increase of the C 1s peak intensity relative to the Cr 2p
52
53
54
55
56
57
58
59
60

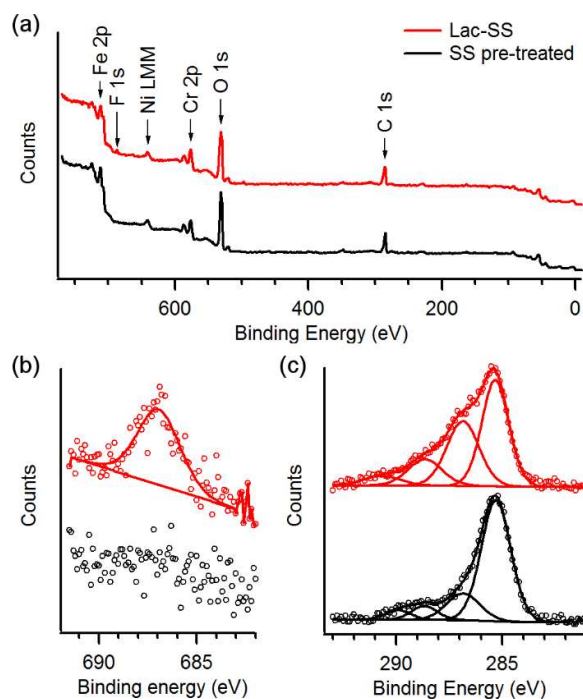


Figure 5. (a) Survey XPS spectra of SS316 after pre-treatment (black) and after modification with F-substituted aryl-lactoside (red). (b) F 1s and (c) C 1s high resolution spectra; these spectra show that upon reaction with aryldiazonium lactosides there appear peak contributions at 687 eV and at 286-289 eV that can be attributed to F-atoms and C—O groups, respectively.

Table 1. Summary of results from XPS analysis of spectra in Figure 5. Values in parentheses indicate %-contribution to the total peak intensity; elemental ratios are calculated as atomic ratios.

	SS pre-treated	Lac-SS
C 1s (eV)	285.3 (70%)	285.1 (46%)
	286.8 (18%)	286.7 (33%)
	288.7 (7%)	288.4 (15%)
	289.9 (5%)	290.5 (6%)
F 1s (eV)	-	687.0
C/Cr at.	6.9	7.6
F/Cr at.	-	0.30
Cr/Fe at.	0.67	0.68

1
2
3 signal, which arises from the substrate alloy. The fit of the C 1s line of Lac-SS (Figure 5c)
4
5 shows (a) the appearance of a contribution at 290.5 eV, consistent with the binding energy
6
7 expected for a C—F group,^{48, 50-51} and (b) increased emission in the region 286-289 eV
8
9 consistent with greater surface density of C—O containing groups and with the presence of
10
11 surface bound glycosides. The RSF corrected peak area ratio $(A_{286}+A_{288}):A_{687} = 12.2$ is in good
12
13 agreement with the 12:1 ratio of C—O to C—F expected from the molecular stoichiometry
14
15 of the fluorinated precursor, thus confirming the assignment of peaks in the region 286-289
16
17 eV to, predominantly, C—O groups from the lactoside, with likely minor contributions from
18
19 substrate carbon. These results therefore indicate that the functionalization protocol
20
21 resulted in surface modification of SS316 with aryl-lactosides.
22
23
24
25

26
27 An estimate of the molecular density can be obtained by assuming that the SS316 substrate
28
29 surface consists of $\text{Cr}_2\text{O}_3/\text{Fe}_2\text{O}_3$ with 40% Cr_2O_3 content ($\text{Cr}/\text{Fe} = 0.67$), as calculated from
30
31 XPS and in agreement with Williams et al.⁴⁶ Considering that both Cr_2O_3 and Fe_2O_3 have a
32
33 density of 5.2 g cm^{-3} , the photoelectron attenuation depth of Cr 2p photoelectrons can be
34
35 predicted to be $\lambda = 1.5 \text{ nm}$ using Gries' G-1 predictive formula.⁵² Under the assumption that
36
37 no photoelectrons escape from depths $>3\lambda$, the average experimental F/Cr 0.17 ± 0.10
38
39 atomic ratio measured over 5 samples yields an estimated mean density of $1.9 \times 10^{-9} \text{ mol cm}^{-2}$.⁵³ For a perfectly smooth surface, this coverage is equivalent to <5 monolayers of
40
41 lactosides.^{30, 54} Given that the microscopic roughness factor of unpolished SS316 is >1 , the
42
43 estimated coverage value suggests the presence of a relatively sparse lactoside layer, as
44
45 expected from a spontaneous reaction of the oxide surface with these bulky aryl-diazonium
46
47 cations and consistent with thin molecular layers formed on carbon substrates via similar
48
49 protocols.³¹
50
51
52
53
54
55
56
57
58
59
60

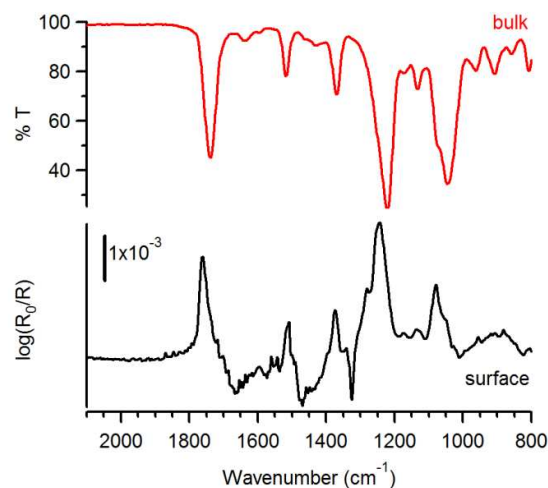
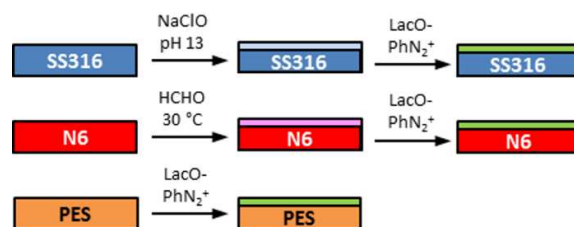


Figure 6. Infrared transmittance spectrum of a peracetylated aminophenol lactoside precursor (red, top) and IRRAS spectrum at 80° incidence of the organic layer obtained after modification of a SS316 sample (black, bottom) with the same aryldiazonium precursor. The IRRAS spectrum displays the characteristic peaks of the precursor compound; peak assignments are discussed in the main text.

Finally, functionalization of SS316 surfaces was confirmed using a peracetylated analog of the aminophenol lactoside precursor (see Scheme 1): acetyl moieties serve as infrared labels thanks to their intense infrared absorbances.³⁰ Figure 6 shows the IRRAS spectrum of a SS316 sample after functionalization (surface, bottom trace), compared to the transmittance spectrum of the peracetylated phenyl-glycoside precursor compound (bulk, top trace).³⁰ The IRRAS spectrum displays the characteristic peaks of acetyl groups at 1760 cm^{-1} (C=O stretching), 1373 cm^{-1} (CH_3 bending) and 1246 cm^{-1} (C-O-C asymmetric stretching).⁵⁵ The peak centered at 1080 cm^{-1} is associated with C-O stretching modes of the carbohydrate ring, while the peak at 1510 cm^{-1} arises from C-C skeletal vibrations of phenyl rings.^{33, 55}

In summary, the functionalization protocol outlined in Scheme 2 was found to be successful at grafting lactoside groups *via* spontaneous reactions of aryldiazonium cations onto SS316



Scheme 2. Protocol used for the modification of SS316, N6 and PES.

and N6 surfaces. To the best of our knowledge this is the first reported protocol for the modification of nylon using aryldiazonium cations. It is interesting to note that the pre-treatment protocol results in the formation of $-OH$ groups and it is therefore likely that the functionalization mechanism involves nucleophilic attack of the hydroxyl onto the electron deficient para position of the aryl ring, in analogy to the S_N1 hydrolysis mechanism of aryldiazonium cations (see Scheme S1).⁵⁶ As regards stainless steel functionalization, most previous reports make use of cathodic electrografting reactions that can be driven even in the presence of a continuous passive oxide.⁵⁷⁻⁵⁹ Small et al.⁶⁰ recently reported on the spontaneous attachment of fluorinated aryldiazonium salts on stainless steel from solution, achieved by polishing samples immediately prior to modification. Mechanical polishing breaks down the steel passive oxide, exposing the iron-rich underlayer which can act as an effective spontaneous reductant in aryldiazonium grafting, in agreement with findings on various oxide-free metals.⁶¹ In our case we have carried out an oxidising pre-treatment which is expected to yield instead a homogeneous hydrophilic passive oxide that cannot directly reduce the aryldiazonium cation; nonetheless, this oxide surface offers a high density of functional $M-OH$ and/or $M-OOH$ sites^{60, 62} available to chemical reaction. There are few reports of spontaneous aryldiazonium reactions on oxides,⁶³⁻⁶⁴ however the spontaneous formation of $M-O-Ar$ bonds has been demonstrated experimentally.⁶⁴ Based

1
2
3 on our results, spontaneous grafting can take place on passivated stainless steel surfaces *via*
4 aryl group cross-linking. It is likely that, as in the case of reactions with primary alcohols,
5 functionalization proceeds *via* nucleophilic substitution involving oxide hydroxyl groups (see
6
7 Scheme S1).⁵⁶
8
9
10

11 12 **Field tests of bare and lactose-modified surfaces**

13
14
15
16 Control and lactose-modified coupons remained immersed in coastal waters for 20 days at
17 the end of which samples were taken out of the water and the amount of biomass
18 accumulated on the coupons was compared using a combination of optical and scanning
19 microscopies, ATP content analysis, IRRAS in the case of SS316 and optical transmission in
20 the case of PES. After immersion minimal differences were observed among different
21 coupon materials, and between lactose-modified samples and unmodified controls of the
22 same material upon visual inspection (Figure S3). However, after controlled light rinsing it
23 was possible to observe clear and significant differences between coated and uncoated
24 samples as discussed below.
25
26
27
28
29
30
31
32
33
34
35
36

37 Figure 7 shows representative optical microscopy images of SS316, nylon-6 and PES coupons
38 positioned at site 1, together with images of a corresponding pristine surface that had not
39 undergone immersion; images of coupons at site 2 showed a similar trend (Figures S4-S6).
40 Samples that had been coated with the aryldiazonium layer of lactoside units were found to
41 display a visibly lower density of foulants. Unmodified samples in Figure 7 (top row) appear
42 to show the evidence of secondary adhesive structures (algae pads or stalks),⁶⁵ which are
43 mostly absent in Lac-modified samples (middle row), and that are important for the
44 development of microbial slimes. Figure 8 shows images at higher resolution obtained by
45
46
47
48
49
50
51
52
53
54
55
56
57
58
59
60

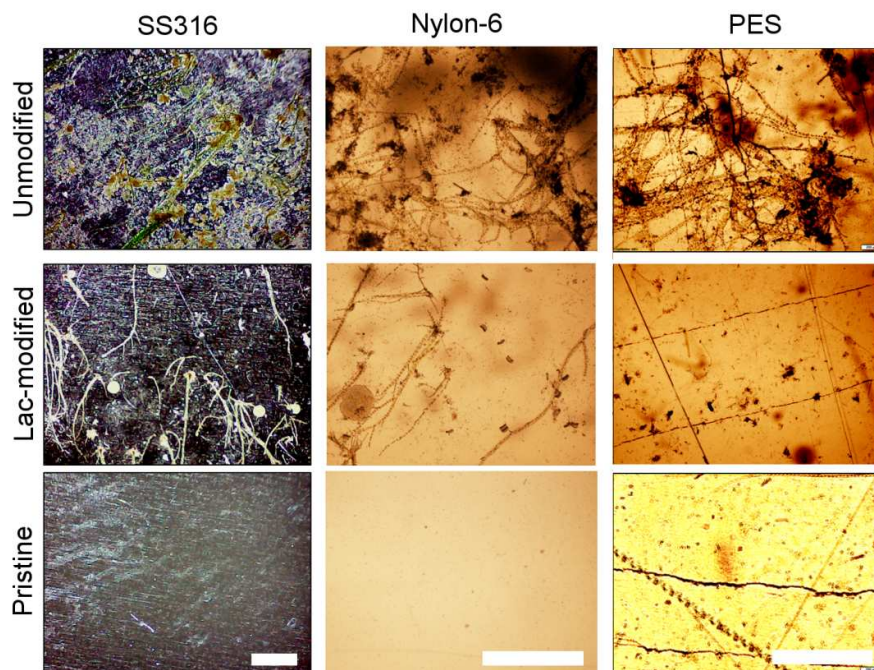


Figure 7. Optical microscope images of coupons of SS316, Nylon-6 and PES (scalebar = 1 mm) extracted after 20 day immersion in coastal waters at site 1 (see Figure 1); samples were rinsed under the same conditions prior to imaging. The top row shows images of coupons that had not been coated with an aryldiazonium layer of glycosides; the middle row shows coupons that had been coated with a layer of lactosides prior to immersion; the bottom row shows samples as supplied by the vendor, without undergoing any immersion tests. All immersed samples display biomass accumulation however the density of adhered organic matter appears to be higher on unmodified when compared to lactoside-modified samples.

SEM and HIM microscopies on SS316 and polymer coupons, respectively. It is possible to observe the presence of diatoms and mucilaginous trails; visual inspection suggests that pennate diatoms dominate the retained deposits, in agreement with typical findings in marine fouling experiments.⁶⁵ Scanning microscopy images also confirmed that a higher density of foulants remained adhered to the unmodified coupons compared to the modified ones for all tested materials.

Total ATP is an indicator of microbial biomass content and can be used to assess biomass accumulation at surfaces.⁶⁶ Samples of known size taken from coupons were immersed into identical volumes of deionized water and sonicated to extract adsorbed biomass; a

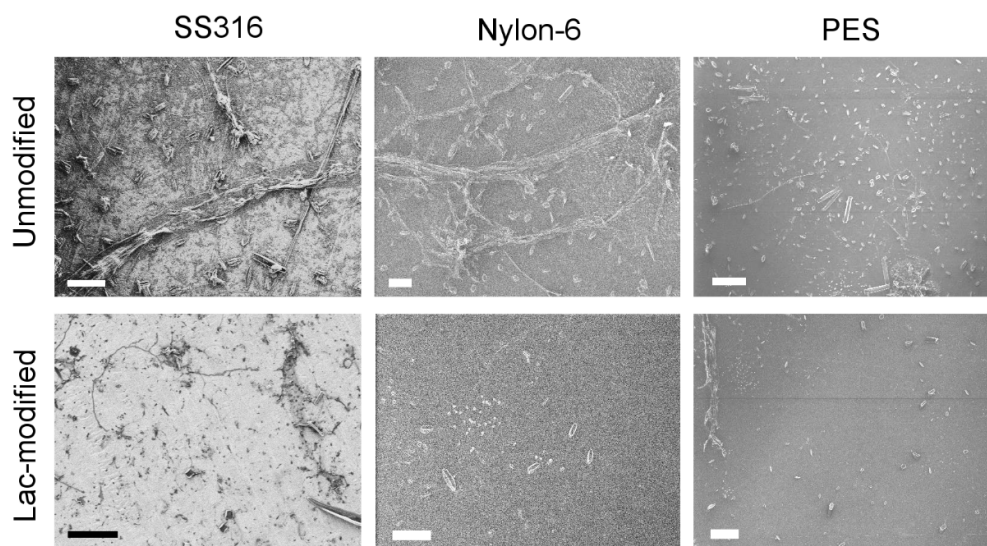


Figure 8. Microscopy images of coupons of SS316 (SEM, scalebar = 40 μm), Nylon-6 (HIM, scalebar = 40 μm) and PES (HIM, scalebar = 100 μm). The figures show details of surfaces after 20 day immersion in coastal waters followed by rinsing under identical conditions prior to imaging. The top row shows images of coupons that had not been coated with an aryldiazonium layer of glycosides; the bottom row shows coupons that had been coated with a layer of lactosides prior to immersion.

commercial bioluminescence assay was used in order to compare the ATP content extracted from control and lactose-modified samples. All RLU values were determined in deionized water and dilution factors were chosen which ensured that measurements fell within the linear dynamic range of the assay;⁶⁷ this procedure allowed for a conversion of RLU values to ATP concentrations in the extract and subsequent conversion to ATP mass released per unit area. Figure 9a shows a summary of ATP determinations obtained for SS316, nylon-6 and PES surfaces after immersion tests and prior to any rinsing. A comparison of ATP values indicates that biofilm accumulation was unaffected by the nature of the substrate material, with similar values obtained for SS316, N6 and PES coupons ($P = 0.18$). ATP values were found to be similar for control and modified coupons; in the case of SS316, results suggest a beneficial effect from the coating ($P = 0.08$) at a slightly higher significance level that might be clarified by further studies with a larger sample size.

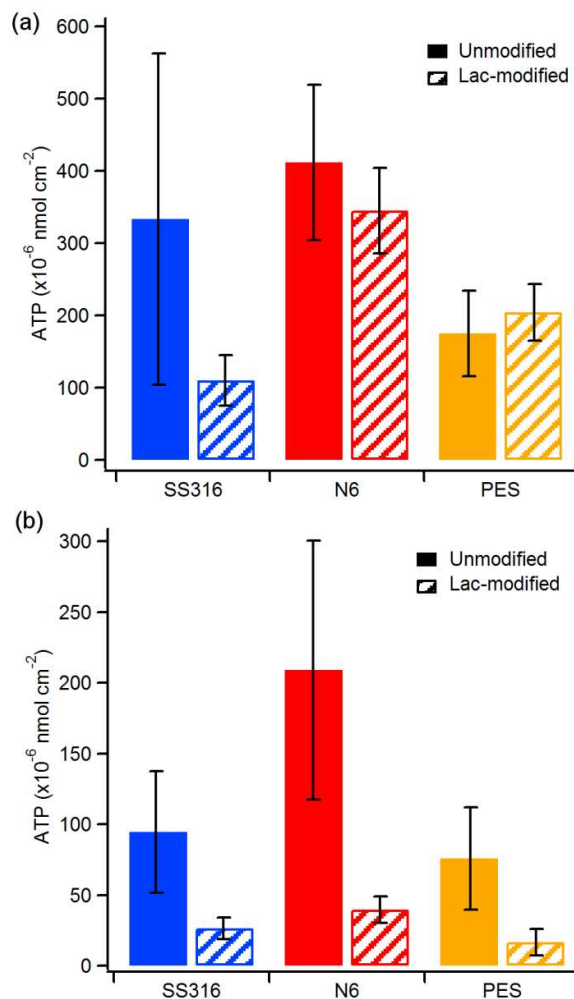


Figure 9. Average ATP released per unit area from unmodified (solid) and lactose-modified (striped) SS316, nylon-6 and PES coupons after 20 day immersion tests in coastal waters prior to any rinsing (a) and after controlled rinsing (b). Error bars indicate 90% C.I.

Figure 9b shows a comparison of ATP values obtained at the three surfaces after controlled rinsing. The level of ATP measured at unmodified (control) surfaces was found to vary depending on the material, with results indicating that nylon-6 retains the highest levels of biomass. A comparison between control and lactose-modified samples clearly shows that surfaces coated by carbohydrate layers have significantly lower amounts of retained biomass; this was confirmed in the case of SS316 ($P = 0.04$), N6 ($P = 0.03$) and PES ($P = 0.04$).

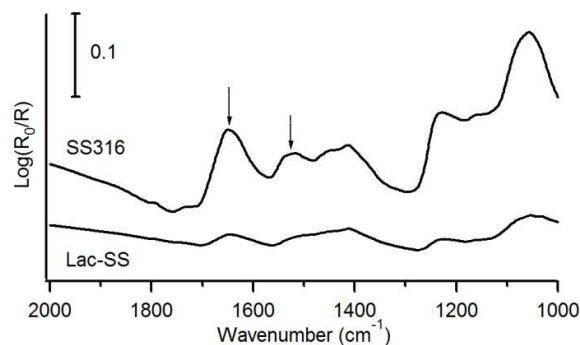


Figure 10. IRRAS spectra at 45° incidence of SS316 unmodified sample and lactose-modified SS316 after 20 day immersion tests; this specific sample was located at site 2 however in all cases unmodified samples show more intense absorption peaks. Arrows indicate peaks at 1645 cm^{-1} and 1525 cm^{-1} corresponding to amide I and amide II modes, respectively.

The controlled rinsing process resulted in a reduction of ATP for all samples, however, the effect is noticeably greater in the case of lactose-modified surfaces yielding reductions of 75%, 89% and 92% for SS316, nylon-6 and PES, respectively. These results therefore indicate that the lactoside layer has a strong impact on the ability of foulants to adhere to the material surface, thus improving resistance to biomass retention; this effect is particularly evident in the case of the two polymers tested.

IRRAS analysis was carried out to compare biomass accumulation at control and modified SS316; this was not possible in the case of N6 and PES due to the poor reflectance of these substrates. Figure 10 shows representative IRRAS spectra in the amide region of both a control and a lactose-modified SS316 sample after rinsing. The spectra show peaks at 1640 cm^{-1} and 1530 cm^{-1} which are assigned to the amide I and amide II modes, respectively, of polypeptides.⁵⁵ These peaks display higher intensity for unmodified SS316, thus indicating that the surface density of proteinaceous material accumulated on control surfaces is higher than on lactose-modified surfaces.

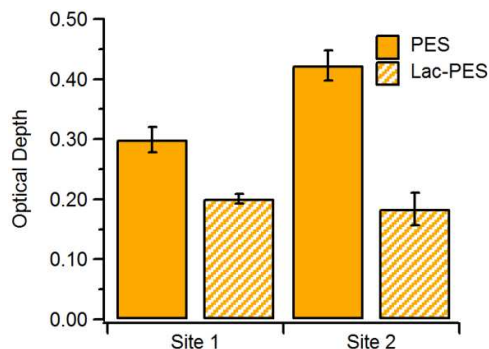


Figure 11. Optical depth of PES coupons at 600 nm measured after 20 day immersion test followed by controlled rinsing. Lac-modified samples are more transparent than unmodified ones.

PES coupons used in our studies were optically transparent, therefore, a quantitative assessment of biomass accumulation could also be obtained through measurements of optical depth ($-\ln(T)$). Figure 11 shows a comparison of the optical depth at 600 nm measured through PES coupons using a pristine PES sample as background: lactose-modified samples were more transparent than unmodified ones, and independently of the site tested, displayed significantly lower optical depth than the corresponding control sample. These results are in agreement with ATP determinations and with microscopy observations.

Carbohydrate layers prepared *via* aryldiazonium chemistry are molecular coatings in the 1-2 nm thickness range that preserve the topography of the original substrate,^{31, 33} so that their main effect is expected to be on surface chemistry and free energy. Results from field experiments show that in the absence of rinsing these coatings do not significantly impact on fouling resistance and little difference is observed with controls. Coupons extracted after the 20 day immersion were significantly fouled by a mixture of organisms and the presence of the coating did not affect marine biofilm formation. However, the accumulated biomass

1
2
3 was dramatically reduced at carbohydrate-modified surfaces after only light rinsing by
4
5 gravity driven streams. SEM and HIM imaging of samples showed that rinsing leaves a
6
7 relatively clean surface, indicating effective detachment of the biofilm under very mild
8
9 treatment. Therefore, these carbohydrate coatings were found to be effective at reducing
10
11 adhesion of foulants on all three materials tested.
12
13

14
15 Recent field tests of coatings based on zwitterionic polymers by Hibbs et al.⁶⁸ resulted in
16
17 similar findings: zwitterionic coatings were found to affect foulant retention after jet rinsing,
18
19 rather than to alter the amount of biomass accumulated on the coupons over the testing
20
21 period. The striking agreement with our trends suggests analogies in the mode of action of
22
23 carbohydrate thin films: these are thought to control fouling by regulating surface
24
25 hydration, which is a similar mechanism to that proposed for zwitterionic polymers,¹ albeit
26
27 in the absence of a change in surface electrostatic charge. It has been proposed that the
28
29 exact distribution of charged regions in zwitterionic coatings might play a role in modulating
30
31 settlement behaviour;⁶⁸ it would be therefore relevant to carry out similar experiments to
32
33 those by Aldred et al.²² on settlement behaviour to investigate whether glycoside structure
34
35 and presentation could be similarly leveraged in carbohydrate coatings.
36
37
38
39
40

41 **Conclusions**

42
43

44 Functionalization and field test results suggest that carbohydrate aryldiazonium layers could
45
46 find applications as fouling resistant coatings. For all materials tested, the density of
47
48 retained biomass at surfaces was found to be significantly lower on carbohydrate modified
49
50 samples with respect to unmodified controls. The mode of action of these layers appears to
51
52 affect biofilm adhesion rather than biofilm formation, operating *via* fouling release rather
53
54 than *via* antifouling mechanisms. It is recognized that fouling minimization in natural
55
56
57
58
59
60

1
2
3 seawaters is extremely challenging due to the presence of multiple organism populations
4
5 with a wide range of adhesion mechanisms. ATP tests suggest that fouling resistance
6
7 observed for lactoside-aryldiazonium layers is comparable to that observed for more
8
9 chemically complex coating systems in laboratory assays, which use populations containing
10
11 a single organism. It is therefore significant that the promising results herein reported were
12
13 obtained in coastal waters, over prolonged times of exposure and during the summer
14
15 months, when fouling activity is maximized.
16
17

18
19 Given the marked differences in physico-chemical properties among SS316 and the two
20
21 polymers it is also encouraging to observe similar trends independent of material, as it
22
23 suggests potential applicability on a variety of devices, including devices consisting of mixed
24
25 materials. Although comprehensive fouling control remains elusive, our experiments
26
27 indicate that thin carbohydrate layers could enhance the effectiveness of other fouling
28
29 control methods. For instance, they could be easily combined/integrated with topography-
30
31 based antifouling strategies, as they coat surfaces conformally with few molecular layers; or
32
33 be combined with mechanical methods to reduce power consumption associated to foulant
34
35 removal. The observed performance, together with the complete absence of toxicity and
36
37 environmental impact of glycan based coatings make them attractive as a sustainable
38
39 fouling mitigation strategy.
40
41
42
43

44 45 **Supporting Information**

46
47 Additional XPS spectra; details of compound synthesis, proposed functionalization
48
49 mechanism; comparison of coupons in the absence of rinsing and immersed at the two
50
51 different sites. This material is available free of charge *via* the Internet at _____.
52
53
54
55
56
57

Corresponding Authors

*E-mail: COLAVITP@tcd.ie; eoin.scanlan@tcd.ie

Funding Sources

This publication has emanated from research conducted with the financial support of Science Foundation Ireland (SFI) grant No. 12/RC/2278 and 12/RC/2302; AM acknowledges support from the School of Chemistry.

Notes

Some of the authors are co-inventors of patent filings covering selected aspects in this article.

Acknowledgements

The authors are grateful to T. McDermott, D. Jackson and F. Kane of the Marine Institute Ireland and Majbritt Bolton-Warberg of Carna Research Station (NUIG) for access to boating equipment and coastal testing facilities. The authors are also grateful to J. Headlam and A. Long (NUIG) for their assistance during the sampling periods. The authors also thank Dr. J. O'Brien, Dr. M. Ruether, Dr. M. Feeney, Dr. G. Hessman and Dr. S.N. Stamatina for assistance with NMR, MS and XPS characterization. The authors acknowledge Advanced Microscopic Laboratory (AML) and D. Daly of Trinity College Dublin for providing access to SEM and HIM.

References

1. Callow, J. A.; Callow, M. E., Trends in the development of environmentally friendly fouling-resistant marine coatings. *Nat. Commun.* **2011**, *2*, 244 DOI: 10.1038/ncomms1251.
2. Fitridge, I.; Dempster, T.; Guenther, J.; de Nys, R., The impact and control of biofouling in marine aquaculture: a review. *Biofouling* **2012**, *28* (7), 649-669 DOI: 10.1080/08927014.2012.700478.

3. Cao, S.; Wang, J.; Chen, H.; Chen, D., Progress of marine biofouling and antifouling technologies. *Chin. Sci. Bull.* **2011**, *56* (7), 598-612 DOI: 10.1007/s11434-010-4158-4.
4. Chambers, L. D.; Stokes, K. R.; Walsh, F. C.; Wood, R. J. K., Modern approaches to marine antifouling coatings. *Surf. Coat. Technol.* **2006**, *201* (6), 3642-3652 DOI: 10.1016/j.surfcoat.2006.08.129.
5. Yebra, D. M.; Kiil, S.; Dam-Johansen, K., Antifouling technology—past, present and future steps towards efficient and environmentally friendly antifouling coatings. *Prog. Org. Coat.* **2004**, *50* (2), 75-104 DOI: 10.1016/j.porgcoat.2003.06.001.
6. Whelan, A.; Regan, F., Antifouling strategies for marine and riverine sensors. *J. Environ. Monit.* **2006**, *8* (9), 880-886 DOI: 10.1039/B603289C.
7. Videla, H. A.; Characklis, W. G., Biofouling and microbially influenced corrosion. *Int. Biodeterior. Biodegradation* **1992**, *29* (3), 195-212 DOI: 10.1016/0964-8305(92)90044-O.
8. Schultz, M. P.; Bendick, J. A.; Holm, E. R.; Hertel, W. M., Economic impact of biofouling on a naval surface ship. *Biofouling* **2011**, *27* (1), 87-98 DOI: 10.1080/08927014.2010.542809.
9. Minchin, D.; Gollasch, S., Fouling and Ships' Hulls: How Changing Circumstances and Spawning Events may Result in the Spread of Exotic Species. *Biofouling* **2003**, *19* (sup1), 111-122 DOI: 10.1080/0892701021000057891.
10. Ruane, N. M.; Rodger, H.; Mitchell, S.; Doyle, T.; Baxter, E.; Fringuelli, E. *GILPAT: An Investigation into Gill Pathologies in Marine Reared Finfish*; Marine Institute: 2013.
11. Carl, C.; Guenther, J.; Sunde, L. M., Larval release and attachment modes of the hydroid *Ectopleura larynx* on aquaculture nets in Norway. *Aquacult. Res.* **2011**, *42* (7), 1056-1060 DOI: 10.1111/j.1365-2109.2010.02659.x.
12. Baxter, E. J.; Sturt, M. M.; Ruane, N. M.; Doyle, T. K.; McAllen, R.; Rodger, H. D., Biofouling of the hydroid *Ectopleura larynx* on aquaculture nets in Ireland: Implications for finfish health. *Fish Vet. J.* **2012**, *13*, 17-29.
13. Magin, C. M.; Cooper, S. P.; Brennan, A. B., Non-toxic antifouling strategies. *Materials Today* **2010**, *13* (4), 36-44 DOI: 10.1016/S1369-7021(10)70058-4.
14. Senda, T.; Miyata, O.; Kihara, T.; Yamada, Y., Inspection Method for the Identification of TBT-containing Antifouling Paints. *Biofouling* **2003**, *19* (sup1), 231-237 DOI: 10.1080/0892701021000057918.
15. Dobretsov, S.; Teplitski, M.; Paul, V., Mini-review: quorum sensing in the marine environment and its relationship to biofouling. *Biofouling* **2009**, *25* (5), 413-427 DOI: 10.1080/08927010902853516.
16. Bixler, G. D.; Bhushan, B., Biofouling: lessons from nature. *Philos. Trans. R. Soc. London, A* **2012**, *370* (1967), 2381-2417 DOI: 10.1098/rsta.2011.0502.

- 1
2
3 17. Schumacher, J. F.; Aldred, N.; Callow, M. E.; Finlay, J. A.; Callow, J. A.; Clare, A. S.;
4 Brennan, A. B., Species-specific engineered antifouling topographies: correlations between
5 the settlement of algal zoospores and barnacle cyprids. *Biofouling* **2007**, *23* (5), 307-317
6 DOI: 10.1080/08927010701393276.
7
- 8 18. Banerjee, I.; Pangule, R. C.; Kane, R. S., Antifouling Coatings: Recent Developments in
9 the Design of Surfaces That Prevent Fouling by Proteins, Bacteria, and Marine Organisms.
10 *Adv. Mater. (Weinheim, Ger.)* **2011**, *23* (6), 690-718 DOI: 10.1002/adma.201001215.
11
- 12 19. Lejars, M.; Margaillan, A.; Bressy, C., Fouling Release Coatings: A Nontoxic
13 Alternative to Biocidal Antifouling Coatings. *Chem. Rev.* **2012**, *112* (8), 4347-4390 DOI:
14 10.1021/cr200350v.
15
- 16 20. Rosenhahn, A.; Schilp, S.; Kreuzer, H. J.; Grunze, M., The role of "inert" surface
17 chemistry in marine biofouling prevention. *Phys. Chem. Chem. Phys.* **2010**, *12* (17), 4275-
18 4286 DOI: 10.1039/C001968M.
19
- 20 21. Kirschner, C. M.; Brennan, A. B., Bio-Inspired Antifouling Strategies. *Annu. Rev.*
21 *Mater. Res.* **2012**, *42* (1), 211-229 DOI: 10.1146/annurev-matsci-070511-155012.
22
- 23 22. Aldred, N.; Li, G.; Gao, Y.; Clare, A. S.; Jiang, S., Modulation of barnacle (*Balanus*
24 *amphitrite* Darwin) cyprid settlement behavior by sulfobetaine and carboxybetaine
25 methacrylate polymer coatings. *Biofouling* **2010**, *26* (6), 673-683 DOI:
26 10.1080/08927014.2010.506677.
27
- 28 23. Perrino, C.; Lee, S.; Choi, S. W.; Maruyama, A.; Spencer, N. D., A Biomimetic
29 Alternative to Poly(ethylene glycol) as an Antifouling Coating: Resistance to Nonspecific
30 Protein Adsorption of Poly(l-lysine)-graft-dextran. *Langmuir* **2008**, *24* (16), 8850-8856 DOI:
31 10.1021/la800947z.
32
- 33 24. Ostuni, E.; Chapman, R. G.; Holmlin, R. E.; Takayama, S.; Whitesides, G. M., A Survey
34 of Structure–Property Relationships of Surfaces that Resist the Adsorption of Protein.
35 *Langmuir* **2001**, *17* (18), 5605-5620 DOI: 10.1021/la010384m.
36
- 37 25. Ederth, T.; Ekblad, T.; Pettitt, M. E.; Conlan, S. L.; Du, C.-X.; Callow, M. E.; Callow, J.
38 A.; Mutton, R.; Clare, A. S.; D'Souza, F.; Donnelly, G.; Bruin, A.; Willemsen, P. R.; Su, X. J.;
39 Wang, S.; Zhao, Q.; Hederos, M.; Konradsson, P.; Liedberg, B., Resistance of Galactoside-
40 Terminated Alkanethiol Self-Assembled Monolayers to Marine Fouling Organisms. *ACS Appl.*
41 *Mater. Interfaces* **2011**, *3* (10), 3890-3901 DOI: 10.1021/am200726a.
42
- 43 26. Luk, Y.-Y.; Kato, M.; Mrksich, M., Self-Assembled Monolayers of Alkanethiolates
44 Presenting Mannitol Groups Are Inert to Protein Adsorption and Cell Attachment. *Langmuir*
45 **2000**, *16* (24), 9604-9608.
46
- 47 27. Hederos, M.; Konradsson, P.; Liedberg, B., Synthesis and Self-Assembly of Galactose-
48 Terminated Alkanethiols and Their Ability to Resist Proteins. *Langmuir* **2005**, *21* (7), 2971-
49 2980 DOI: 10.1021/la047203b.
50
- 51
52
53
54
55
56
57
58
59
60

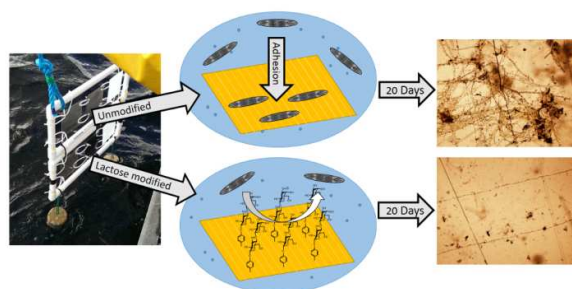
- 1
2
3 28. Cao, X.; Pettit, M. E.; Conlan, S. L.; Wagner, W.; Ho, A. D.; Clare, A. S.; Callow, J. A.;
4 Callow, M. E.; Grunze, M.; Rosenhahn, A., Resistance of Polysaccharide Coatings to Proteins,
5 Hematopoietic Cells, and Marine Organisms. *Biomacromolecules* **2009**, *10* (4), 907-915 DOI:
6 10.1021/bm8014208.
7
- 8 29. Nurioglu, A. G.; Esteves, A. C. C.; de With, G., Non-toxic, non-biocide-release
9 antifouling coatings based on molecular structure design for marine applications. *J. Mater.*
10 *Chem. B* **2015**, *3* (32), 6547-6570 DOI: 10.1039/C5TB00232J.
11
- 12 30. Jayasundara, D. R.; Duff, T.; Angione, M. D.; Bourke, J.; Murphy, D. M.; Scanlan, E.
13 M.; Colavita, P. E., Carbohydrate Coatings via Aryldiazonium Chemistry for Surface
14 Biomimicry. *Chem. Mater.* **2013**, *25* (20), 4122-4128 DOI: 10.1021/cm4027896.
15
- 16 31. Zen, F.; Angione, M. D.; Behan, J. A.; Cullen, R. J.; Duff, T.; Vasconcelos, J. M.;
17 Scanlan, E. M.; Colavita, P. E., Modulation of Protein Fouling and Interfacial Properties at
18 Carbon Surfaces via Immobilization of Glycans Using Aryldiazonium Chemistry. *Sci. Rep.*
19 **2016**, *6*, 24840 DOI: 10.1038/srep24840.
20
- 21 32. Esteban-Tejeda, L.; Duff, T.; Ciapetti, G.; Daniela Angione, M.; Myles, A.; Vasconcelos,
22 J. M.; Scanlan, E. M.; Colavita, P. E., Stable hydrophilic poly(dimethylsiloxane) via glycan
23 surface functionalization. *Polymer* **2016**, *106*, 1-7 DOI: 10.1016/j.polymer.2016.10.044.
24
- 25 33. Angione, M. D.; Duff, T.; Bell, A. P.; Stamatin, S. N.; Fay, C.; Diamond, D.; Scanlan, E.
26 M.; Colavita, P. E., Enhanced Antifouling Properties of Carbohydrate Coated Poly(ether
27 sulfone) Membranes. *ACS Appl. Mater. Interfaces* **2015**, *7* (31), 17238-17246 DOI:
28 10.1021/acsami.5b04201.
29
- 30 34. Mandrino, D.; Godec, M.; Torkar, M.; Jenko, M., Study of oxide protective layers on
31 stainless steel by AES, EDS and XPS. *Surf. Interface Anal.* **2008**, *40* (3-4), 285-289 DOI:
32 10.1002/sia.2718.
33
- 34 35. Hassel, M.; Hemmerich, I.; Kuhlenbeck, H.; Freund, H.-J., High Resolution XPS Study
35 of a Thin Cr₂O₃(111) Film Grown on Cr(110). *Surf. Sci. Spectra* **1996**, *4* (3), 246-252 DOI:
36 10.1116/1.1247795.
37
- 38 36. Beeskow, T.; Kroner, K. H.; Anspach, F. B., Nylon-Based Affinity Membranes: Impacts
39 of Surface Modification on Protein Adsorption. *J. Colloid Interface Sci.* **1997**, *196* (2), 278-
40 291 DOI: 10.1006/jcis.1997.5199.
41
- 42 37. Railkin, A. I., *Marine Biofouling: Colonization Processes and Defenses*. CRC Press:
43 2003.
44
- 45 38. Tanane, O.; Abboud, Y.; Aitenneite, H.; El Bouari, A., Corrosion inhibition of the 316L
46 stainless steel in sodium hypochlorite media by sodium silicate. *J. Mater. Environ. Sci.* **2016**,
47 *7* (1), 131-13.
48
- 49 39. Lins, V. d. F. C.; Gonçalves, G. A. d. S.; Leão, T. P.; Soares, R. B.; Costa, C. G. F.; Viana,
50 A. K. d. N., Corrosion resistance of AISI 304 and 444 stainless steel pipes in sanitizing
51 solutions of clean-in-place process. *Mat. Res.* **2016**, *19*, 333-338.
52
53
54
55
56
57
58
59
60

- 1
2
3 40. Pierozynski, B.; Kowalski, I., The Influence of Hypochlorite-Based Disinfectants on the
4 Pitting Corrosion of Welded Joints of 316L Stainless Steel Dairy Reactor. *Int. J. Electrochem.*
5 *Sci.* **2011**, *6*, 3913-392.
6
- 7 41. Cairns, T. L.; Foster, H. D.; Larchar, A. W.; Schneider, A. K.; Schreiber, R. S.,
8 Preparation and Properties of N-Methylol, N-Alkoxyethyl and N-Alkylthiomethyl
9 Polyamides. *J. Am. Chem. Soc.* **1949**, *71* (2), 651-655 DOI: 10.1021/ja01170a074.
10
- 11 42. Lin, J.; Winkelman, C.; Worley, S. D.; Broughton, R. M.; Williams, J. F., Antimicrobial
12 treatment of nylon. *J. Appl. Polym. Sci.* **2001**, *81* (4), 943-947 DOI: 10.1002/app.1515.
13
- 14 43. Tang, S.; Lu, N.; Myung, S.-W.; Choi, H.-S., Enhancement of adhesion strength
15 between two AISI 316 L stainless steel plates through atmospheric pressure plasma
16 treatment. *Surf. Coat. Technol.* **2006**, *200* (18-19), 5220-5228 DOI:
17 10.1016/j.surfcoat.2005.06.020.
18
- 19 44. Maupin, K. A.; Liden, D.; Haab, B. B., The fine specificity of mannose-binding and
20 galactose-binding lectins revealed using outlier motif analysis of glycan array data.
21 *Glycobiology* **2012**, *22* (1), 160-169 DOI: 10.1093/glycob/cwr128.
22
- 23 45. Hryniewicz, T.; Rokosz, K.; Rokicki, R., Electrochemical and XPS studies of AISI 316L
24 stainless steel after electropolishing in a magnetic field. *Corros. Sci.* **2008**, *50* (9), 2676-2681
25 DOI: 10.1016/j.corsci.2008.06.048.
26
- 27 46. Williams, D. F.; Kellar, E. J. C.; Jesson, D. A.; Watts, J. F., Surface analysis of 316
28 stainless steel treated with cold atmospheric plasma. *Appl. Surf. Sci.* **2017**, *403* (Supplement
29 C), 240-247 DOI: 10.1016/j.apsusc.2017.01.150.
30
- 31 47. Saulou, C.; Despax, B.; Raynaud, P.; Zanna, S.; Marcus, P.; Mercier-Bonin, M., Plasma-
32 Mediated Modification of Austenitic Stainless Steel: Application to the Prevention of Yeast
33 Adhesion. *Plasma Processes Polym.* **2009**, *6* (12), 813-824 DOI: 10.1002/ppap.200900069.
34
- 35 48. Dilks, A.; Kay, E., Plasma polymerization of ethylene and the series of
36 fluoroethylenes: plasma effluent mass spectrometry and ESCA studies. *Macromolecules*
37 **1981**, *14* (3), 855-862 DOI: 10.1021/ma50004a074.
38
- 39 49. Ferrara, A. M.; Lopes da Silva, J. D.; Botelho do Rego, A. M., XPS studies of directly
40 fluorinated HDPE: problems and solutions. *Polymer* **2003**, *44* (23), 7241-7249 DOI:
41 10.1016/j.polymer.2003.08.038.
42
- 43 50. Golub, M. A.; Wydeven, T.; Johnson, A. L., Similarity of Plasma-Polymerized
44 Tetrafluoroethylene and Fluoropolymer Films Deposited by rf Sputtering of
45 Poly(tetrafluoroethylene). *Langmuir* **1998**, *14* (8), 2217-2220 DOI: 10.1021/la971102e.
46
- 47 51. Gu, X.; Nemoto, T.; Teramoto, A.; Ito, T.; Ohmi, T., Effect of Additives in Organic Acid
48 Solutions for Post-CMP Cleaning on Polymer Low-k Fluorocarbon. *J. Electrochem. Soc.* **2009**,
49 *156* (6), H409-H415 DOI: 10.1149/1.3106106.
50
51
52
53
54
55
56
57
58
59
60

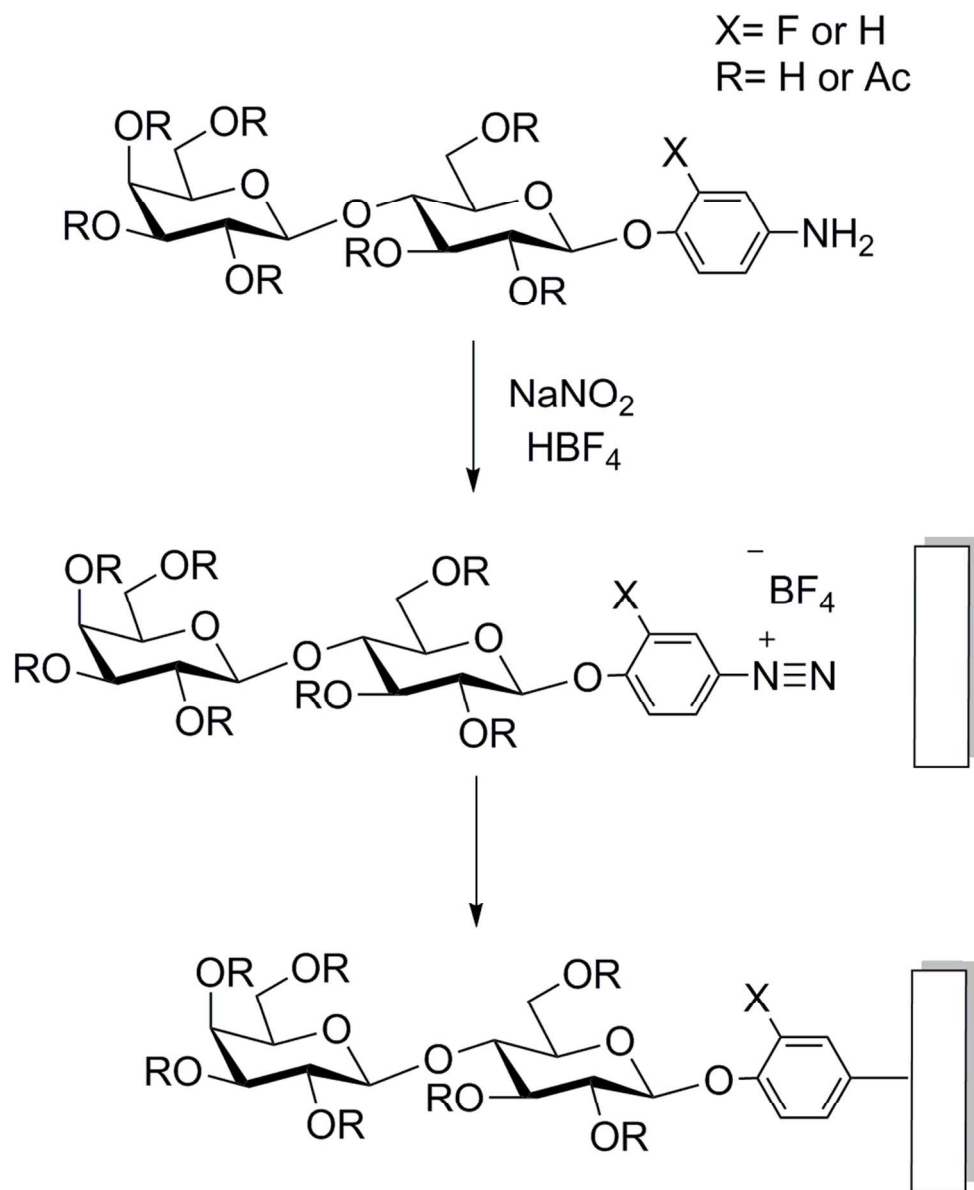
- 1
2
3 52. Powell, C. J.; Jablonski, A., NIST Electron Inelastic-Mean-Free-Path Database, Version
4 1.2. In *NIST Standard Reference Database*, National Institute of Standards and Technology:
5 Gaithersburgh, MD, 2010; Vol. 71.
6
- 7 53. Nichols, B. M.; Butler, J. E.; Russell, J. N.; Hamers, R. J., Photochemical
8 Functionalization of Hydrogen-Terminated Diamond Surfaces: A Structural and Mechanistic
9 Study. *J. Phys. Chem. B* **2005**, *109* (44), 20938-20947 DOI: 10.1021/jp0545389.
10
- 11 54. Hinz, H. J.; Kutenreich, H.; Meyer, R.; Renner, M.; Freund, R.; Koynova, R.; Boyanov,
12 A.; Tenchov, B., Stereochemistry and size of sugar head groups determine structure and
13 phase behavior of glycolipid membranes: densitometric, calorimetric, and x-ray studies.
14 *Biochemistry* **1991**, *30* (21), 5125-5138 DOI: 10.1021/bi00235a003.
15
- 16 55. Socrates, G., *Infrared and Raman Characteristic Group Frequencies: Tables and*
17 *Charts*. John Wiley & Sons: 2001.
18
- 19 56. García Martínez, A.; de la Moya Cerero, S.; Osío Barcina, J.; Moreno Jiménez, F.; Lora
20 Maroto, B., The Mechanism of Hydrolysis of Aryldiazonium Ions Revisited: Marcus Theory
21 vs. Canonical Variational Transition State Theory. *Eur. J. Org. Chem.* **2013**, *2013* (27), 6098-
22 6107 DOI: 10.1002/ejoc.201300834.
23
- 24 57. Hinge, M.; Gonçalves, E. S.; Pedersen, S. U.; Daasbjerg, K., On the electrografting of
25 stainless steel from para-substituted aryldiazonium salts and the thermal stability of the
26 grafted layer. *Surf. Coat. Technol.* **2010**, *205* (3), 820-827 DOI:
27 10.1016/j.surfcoat.2010.07.125.
28
- 29 58. Hinge, M.; Ceccato, M.; Kingshott, P.; Besenbacher, F.; Pedersen, S. U.; Daasbjerg, K.,
30 Electrochemical modification of chromium surfaces using 4-nitro- and 4-
31 fluorobenzenediazonium salts. *New J. Chem.* **2009**, *33* (12), 2405-2408 DOI:
32 10.1039/B9NJ00422J.
33
- 34 59. Le, X. T.; Zeb, G.; Jégou, P.; Berthelot, T., Electrografting of stainless steel by the
35 diazonium salt of 4-aminobenzylphosphonic acid. *Electrochim. Acta* **2012**, *71*, 66-72 DOI:
36 10.1016/j.electacta.2012.03.076.
37
- 38 60. Small, L. J.; Hibbs, M. R.; Wheeler, D. R., Spontaneous Aryldiazonium Film Formation
39 on 440C Stainless Steel in Nonaqueous Environments. *Langmuir* **2014**, *30* (47), 14212-14218
40 DOI: 10.1021/la503630f.
41
- 42 61. Adenier, A.; Barré, N.; Cabet-Deliry, E.; Chaussé, A.; Griveau, S.; Mercier, F.; Pinson,
43 J.; Vautrin-UI, C., Study of the spontaneous formation of organic layers on carbon and metal
44 surfaces from diazonium salts. *Surf. Sci.* **2006**, *600* (21), 4801-4812 DOI:
45 10.1016/j.susc.2006.07.061.
46
- 47 62. Maurice, V.; Cadot, S.; Marcus, P., Hydroxylation of ultra-thin films of α -Cr₂O₃(0001)
48 formed on Cr(110). *Surf. Sci.* **2001**, *471* (1-3), 43-58 DOI: 10.1016/S0039-6028(00)00880-3.
49
50
51
52
53
54
55
56
57
58
59
60

- 1
2
3 63. Dechézelles, J.-F.; Griffete, N.; Dietsch, H.; Scheffold, F., A General Method to Label
4 Metal Oxide Particles with Fluorescent Dyes Using Aryldiazonium Salts. *Part. Part. Syst.*
5 *Charact.* **2013**, *30* (7), 579-583 DOI: 10.1002/ppsc.201300014.
6
7 64. Hurley, B. L.; McCreery, R. L., Covalent Bonding of Organic Molecules to Cu and Al
8 Alloy 2024 T3 Surfaces via Diazonium Ion Reduction. *J. Electrochem. Soc.* **2004**, *151* (5),
9 B252-B259 DOI: 10.1149/1.1687428.
10
11 65. Molino, P. J.; Wetherbee, R., The biology of biofouling diatoms and their role in the
12 development of microbial slimes. *Biofouling* **2008**, *24* (5), 365-379 DOI:
13 10.1080/08927010802254583.
14
15 66. Karl, D. M., Total microbial biomass estimation derived from the measurement of
16 particulate adenosine-5'-triphosphate. In *Handbook of methods in aquatic microbial*
17 *ecology*, Kemp, P. F.; Cole, J. J.; Sherr, B. F.; Sherr, E. B., Eds. Lewis Publishers: Boca Raton ;,
18 1993; pp 359-368.
19
20 67. Omidbakhsh, N.; Ahmadpour, F.; Kenny, N., How Reliable Are ATP Bioluminescence
21 Meters in Assessing Decontamination of Environmental Surfaces in Healthcare Settings? .
22 *PLoS One* **2014**, *9* (6), e99951 DOI: 10.1371/journal.pone.0099951.
23
24 68. Hibbs, M. R.; Hernandez-Sanchez, B. A.; Daniels, J.; Staflien, S. J., Polysulfone and
25 polyacrylate-based zwitterionic coatings for the prevention and easy removal of marine
26 biofouling. *Biofouling* **2015**, *31* (7), 613-624 DOI: 10.1080/08927014.2015.1081179.
27
28
29
30
31
32
33
34
35
36
37
38
39
40
41
42
43
44
45
46
47
48
49
50
51
52
53
54
55
56
57
58
59
60

For Table of Contents Use Only



Ultra-thin saccharide layers offer a non-biocidal, sustainable fouling mitigation strategy.



45
46
47
48
49
50
51
52
53
54
55
56
57
58
59
60

Scheme 1. 4-aminophenol- β -D-lactopyranose compounds used for all functionalized samples and reaction protocol used for diazotization and functionalization with aryldiazonium cations in situ.

87x106mm (300 x 300 DPI)

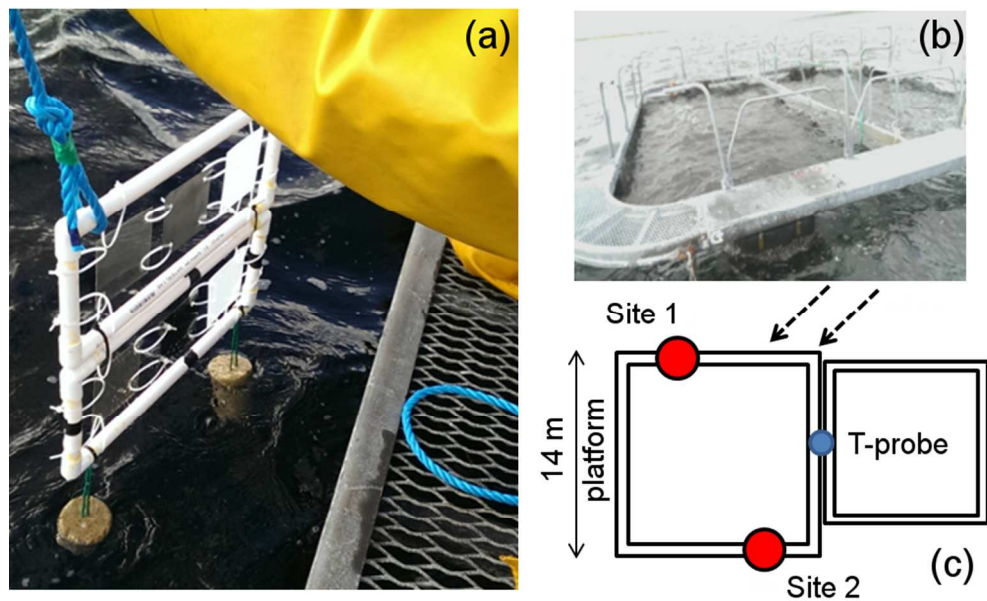


Figure 1. (a) Assembled frame with coupons, arranged from left to right, PES, SS316 and N6, immediately prior to immersion in sea water. (b) Salmon farm platform from which frames with coupons were suspended. (c) Scheme showing the two adjacent platforms and the location of frames at Site 1 and Site 2 relative to the tide (dashed arrows); a temperature probe measured surface water temperature at the position indicated in blue.

86x52mm (300 x 300 DPI)

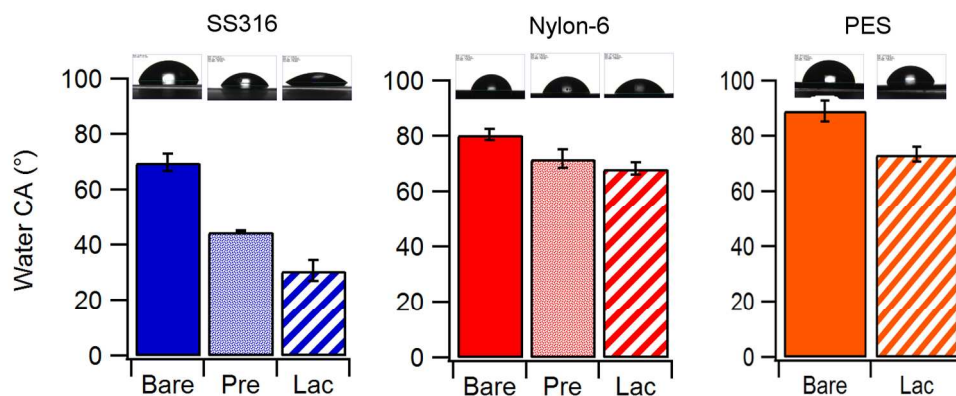
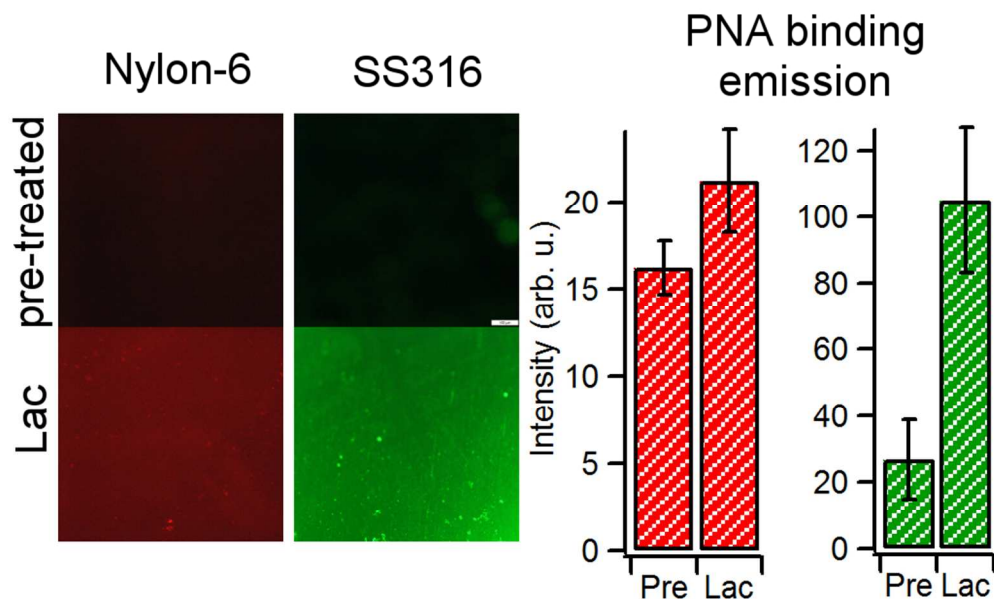


Figure 2. Water contact angle values obtained on bare, pre-treated (except for PES) and Lactose-modified (Lac) surfaces of SS316, Nylon-6 and PES. Samples were pre-activated in caustic bleach and formaldehyde solutions in the case of SS316 and nylon-6, respectively.

159x66mm (300 x 300 DPI)



27 **Figure 3.** Fluorescence images obtained after lectin binding experiments using dye-conjugated PNA on
28 Nylon-6 and SS316 after pre-treatment and after aryldiazonium modification with lactosides (Lac). The
29 images show that the emission intensity is higher on lactose-modified surfaces. Bar plots represent average
30 emission intensities of Alexa-PNA on Nylon-6 (red bars) and of FITC-PNA on SS316 (green bars) obtained at
31 pre-treated (Pre) and at lactose-modified coupons (Lac).

32 87x53mm (300 x 300 DPI)

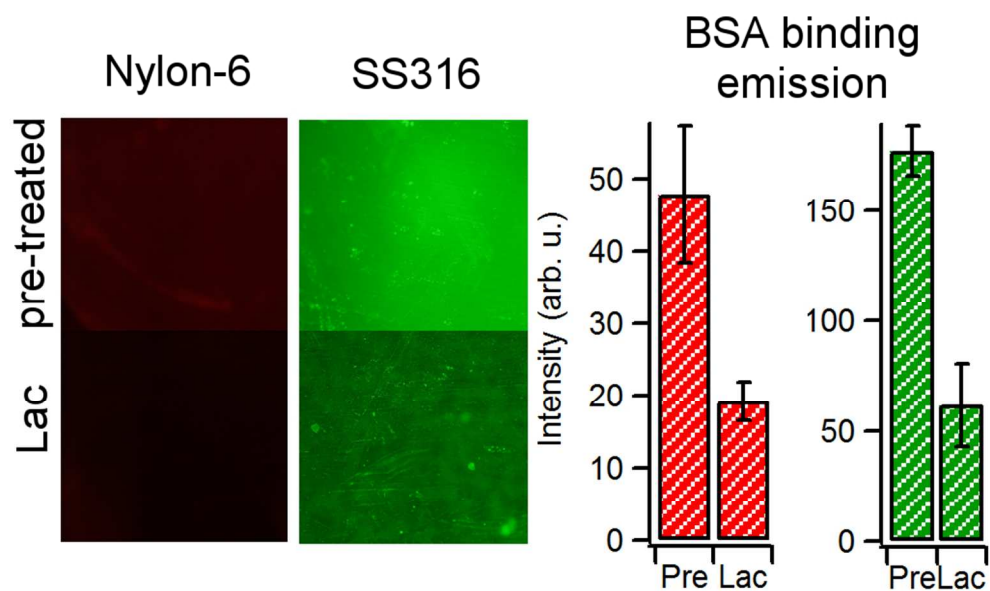


Figure 4. Fluorescence images obtained after protein adsorption experiments using dye-conjugated BSA on Nylon-6 and SS316 after pre-treatment and after aryldiazonium modification with lactosides (Lac). The images show that the emission intensity is lower on lactose-modified surfaces. Bar plots represent average emission intensities of Alexa-BSA on Nylon-6 (red bars) and of FITC-BSA on SS316 (green bars) obtained at pre-treated (Pre) and at lactose-modified coupons (Lac).

87x52mm (300 x 300 DPI)

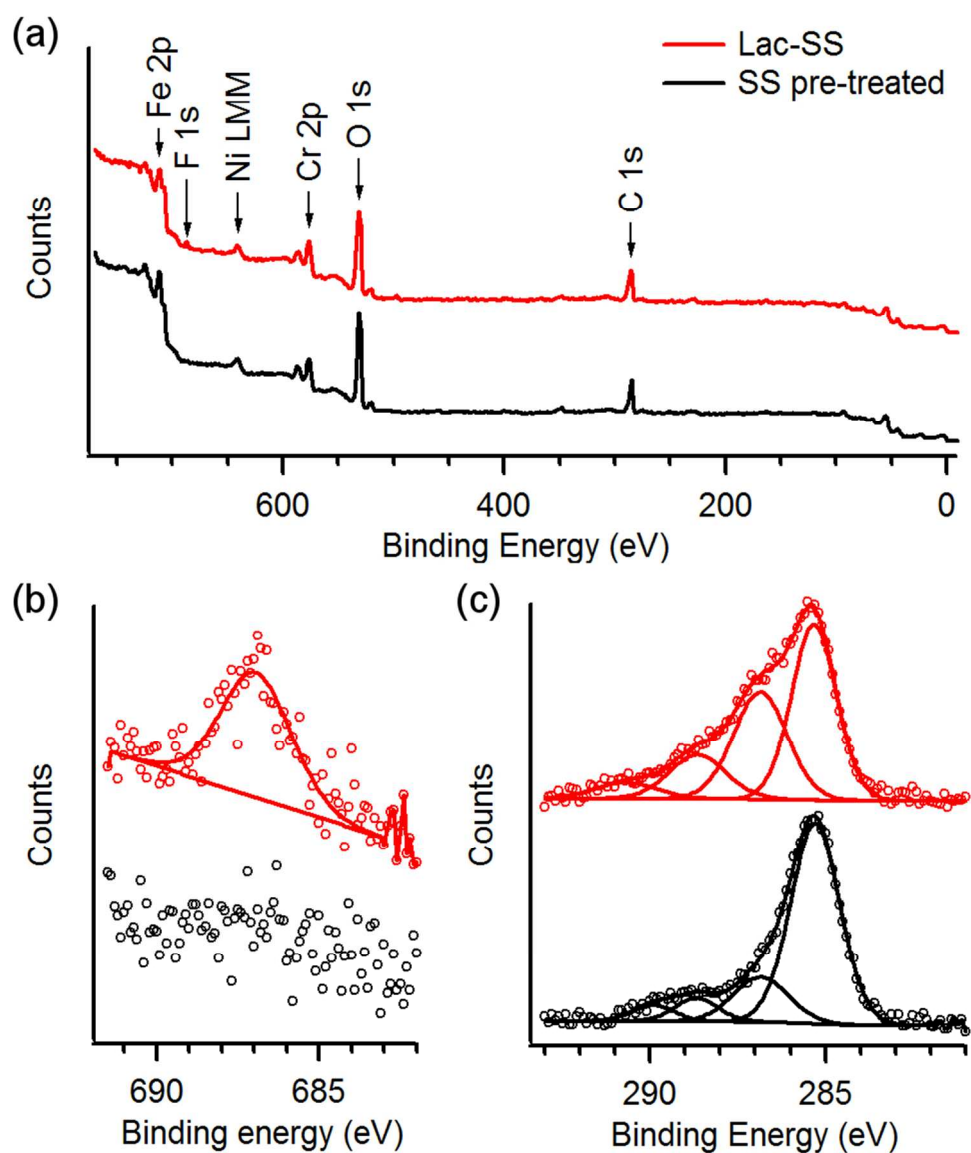


Figure 5. (a) Survey XPS spectra of SS316 after pre-treatment (black) and after modification with F-substituted aryl-lactoside (red). (b) F 1s and (c) C 1s high resolution spectra; these spectra show that upon reaction with aryldiazonium lactosides there appear peak contributions at 687 eV and at 286-289 eV that can be attributed to F-atoms and C—O groups, respectively.

84x99mm (300 x 300 DPI)

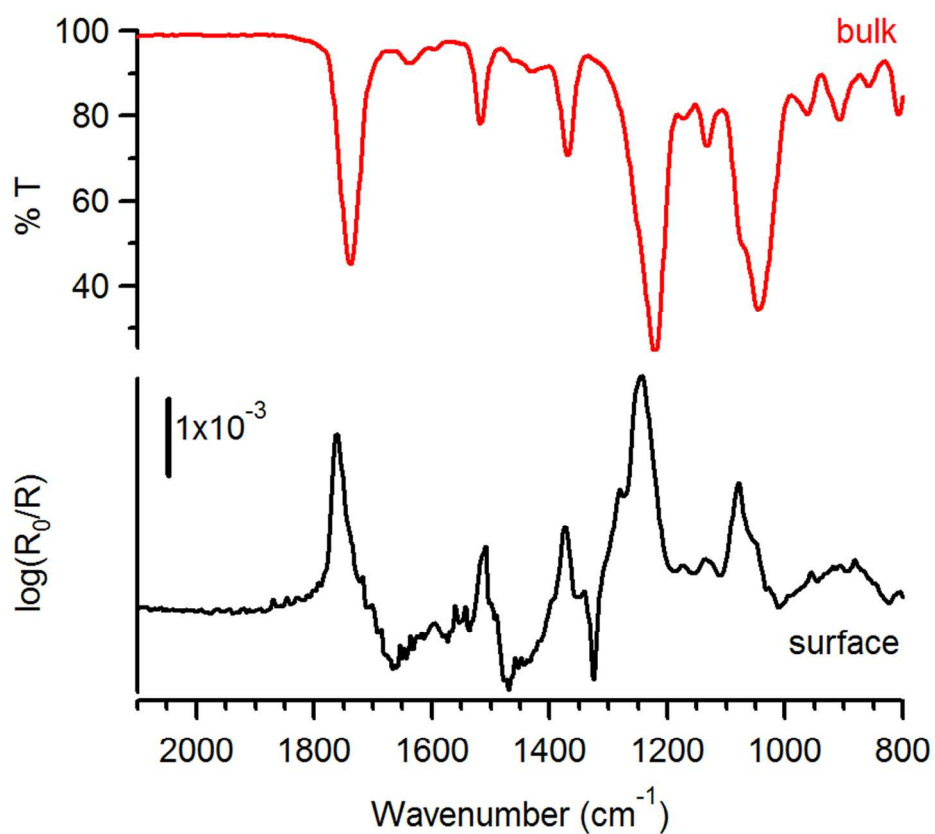
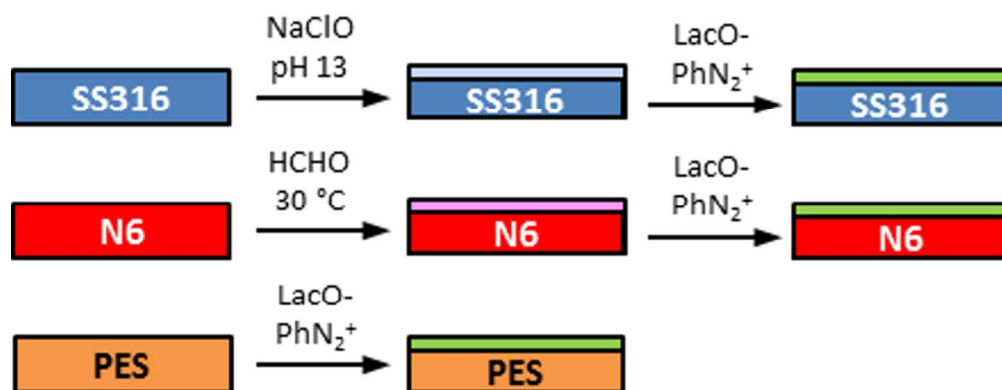


Figure 6. Infrared transmittance spectrum of a peracetylated aminophenol lactoside precursor (red, top) and IRRAS spectrum at 80° incidence of the organic layer obtained after modification of a SS316 sample (black, bottom) with the same aryldiazonium precursor. The IRRAS spectrum displays the characteristic peaks of the precursor compound; peak assignments are discussed in the main text.

81x69mm (300 x 300 DPI)



Scheme 2. Protocol used for the modification of SS316, N6 and PES.

80x30mm (300 x 300 DPI)

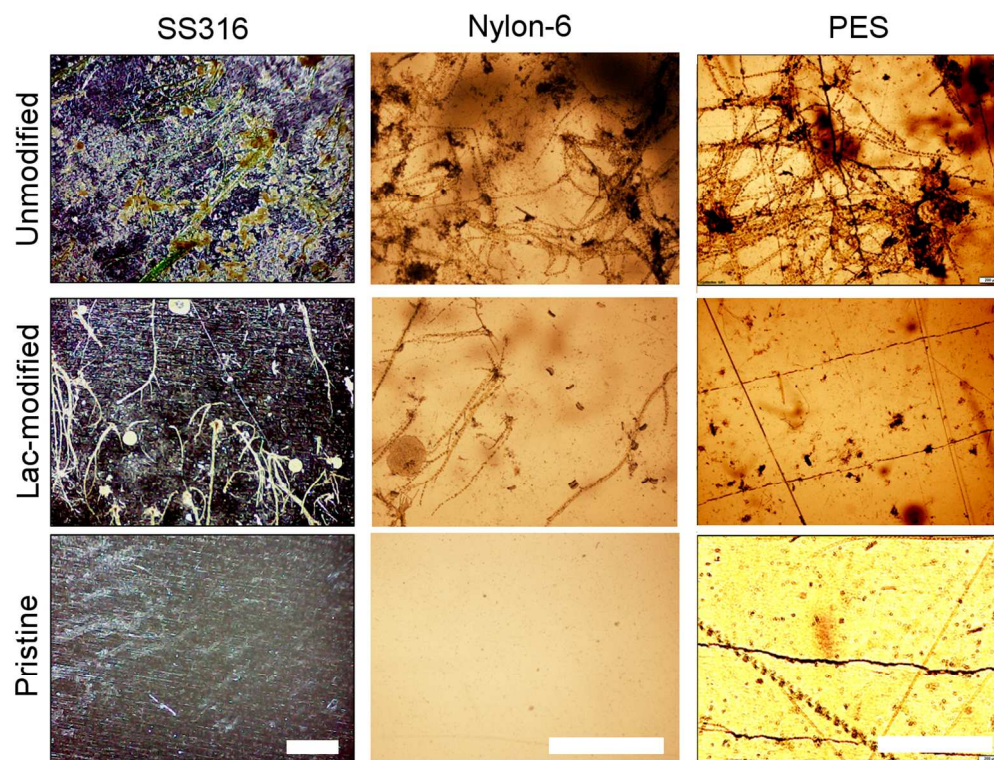
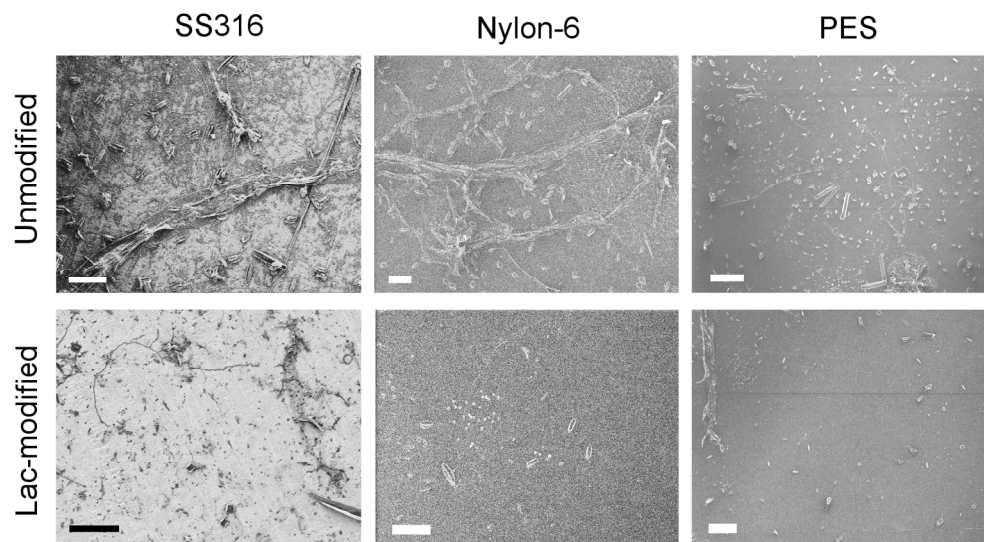


Figure 7. Optical microscope images of coupons of SS316, Nylon- and PES (scalebar = 1 mm) extracted after 20 day immersion in coastal waters at site 1 (see Figure 1); samples were rinsed under the same conditions prior to imaging. The top row shows images of coupons that had not been coated with an aryldiazonium layer of glycosides; the middle row shows coupons that had been coated with a layer of lactosides prior to immersion; the bottom row shows samples as supplied by the vendor, without undergoing any immersion tests. All immersed samples display biomass accumulation however the density of adhered organic matter appears to be higher on unmodified when compared to lactoside-modified samples.

124x95mm (300 x 300 DPI)



25 **Figure 8.** Microscopy images of coupons of SS316 (SEM, scalebar = 40 μm), Nylon-6 (HIM, scalebar = 40
26 μm) and PES (HIM, scalebar = 100 μm). The figures show details of surfaces after 20 day immersion in
27 coastal waters followed by rinsing under identical conditions prior to imaging. The top row shows images of
28 coupons that had not been coated with an aryldiazonium layer of glycosides; the bottom row shows coupons
29 that had been coated with a layer of lactosides prior to immersion.

30 141x78mm (300 x 300 DPI)

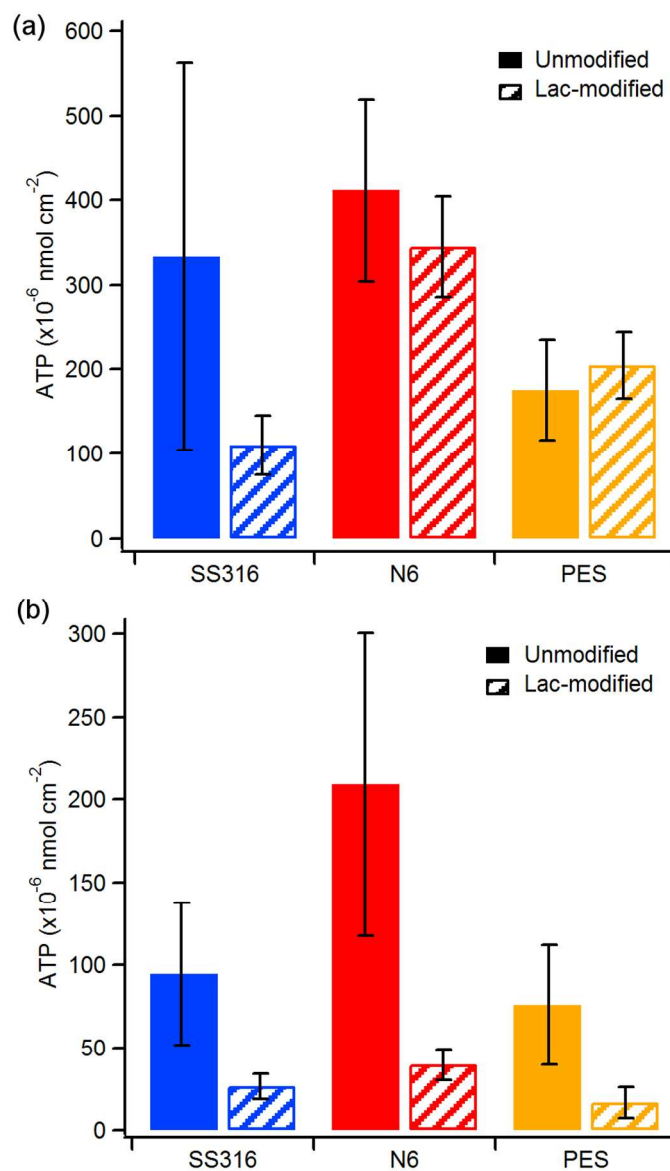


Figure 9. Average ATP released per unit area from unmodified (solid) and lactose-modified (striped) SS316, nylon-6 and PES coupons after 20 day immersion tests in coastal waters prior to any rinsing (a) and after controlled rinsing (b). Error bars indicate 90% C.I.

84x144mm (300 x 300 DPI)

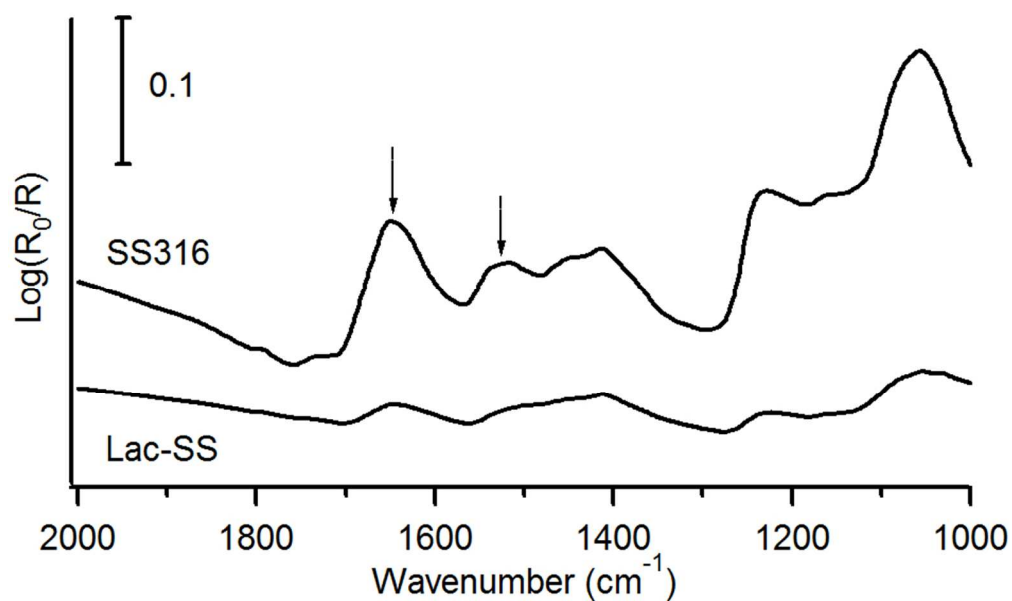


Figure 10. IRRAS spectra at 45° incidence of SS316 unmodified sample and lactose-modified SS316 after 20 day immersion tests; this specific sample was located at site 2 however in all cases unmodified samples show more intense absorption peaks. Arrows indicate peaks at 1645 cm^{-1} and 1525 cm^{-1} corresponding to amide I and amide II modes, respectively.

80x50mm (300 x 300 DPI)

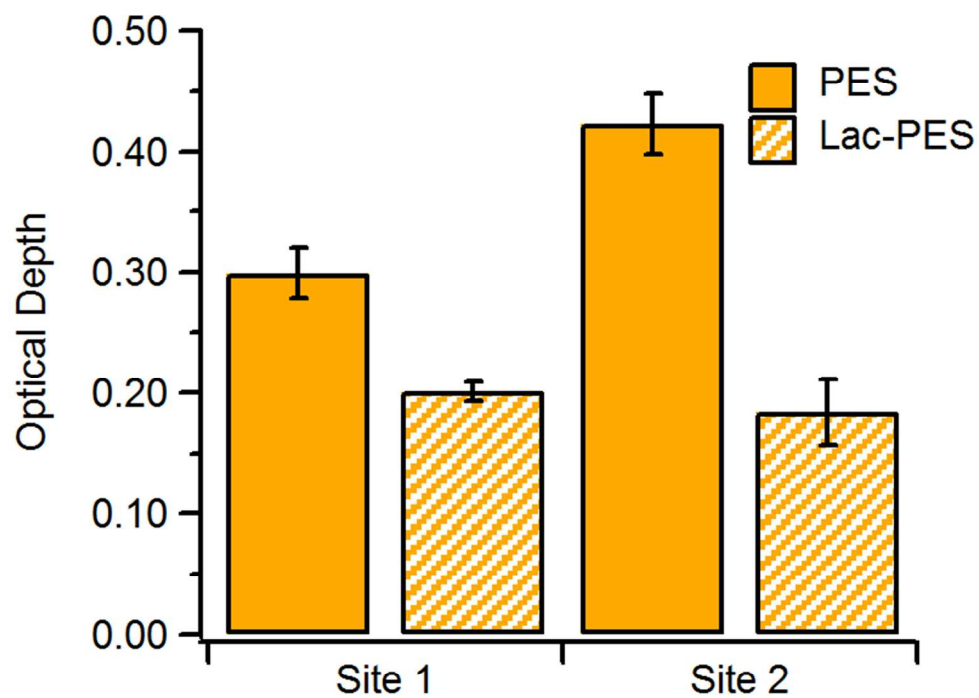
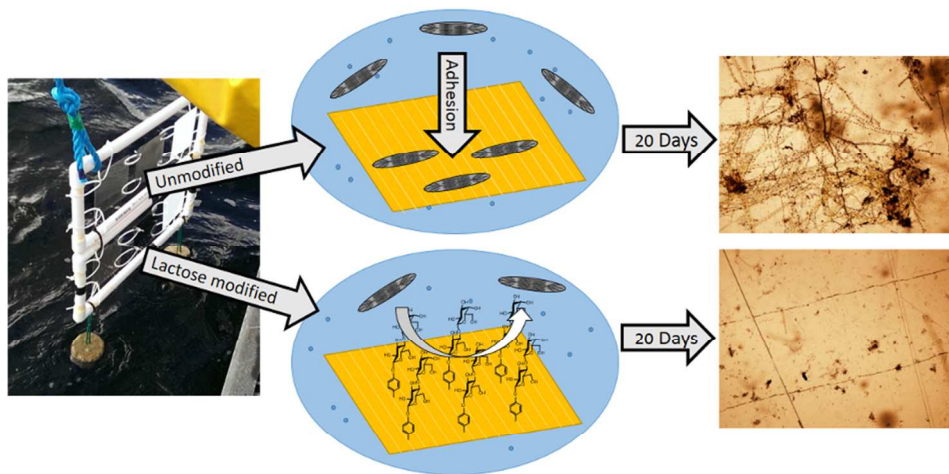


Figure 11. Optical depth of PES coupons at 600 nm measured after 20 day immersion test followed by controlled rinsing. Lac-modified samples are more transparent than unmodified ones.

69x55mm (300 x 300 DPI)

1
2
3
4
5
6
7
8
9
10
11
12
13
14
15
16
17
18
19
20
21
22
23
24
25
26
27
28
29
30
31
32
33
34
35
36
37
38
39
40
41
42
43
44
45
46
47
48
49
50
51
52
53
54
55
56
57
58
59
60



Ultra-thin saccharide layers offer a non-biocidal, sustainable fouling mitigation strategy.

84x47mm (300 x 300 DPI)